JOURNAL OF GEOPHYSICAL RESEARCH, VOL. 108, NO. D19, 8171, doi:10.1029/2002JD002559, 2003

Climate change and Arctic ecosystems: 2. Modeling, paleodata-model comparisons, and future projections

J. O. Kaplan,[1,2,3] N. H. Bigelow,[4] I. C. Prentice,[1] S. P. Harrison,[1,5] P. J. Bartlein,[6] T. R. Christensen,[7,8] W. Cramer,[9] N. V. Matveyeva,[10] A. D. McGuire,[11] D. F. Murray,[12] V. Y. Razzhivin,[10] B. Smith,[1,7,8] D. A. Walker,[13,14] P. M. Anderson,[15] A. A. Andreev,[16] L. B. Brubaker,[17] M. E. Edwards,[14,18,19] and A. V. Lozhkin[20]

Received 23 May 2002; revised 6 January 2003; accepted 29 January 2003; published 8 October 2003.

[1] Large variations in the composition, structure, and function of Arctic ecosystems are determined by climatic gradients, especially of growing-season warmth, soil moisture, and snow cover. A unified circumpolar classification recognizing five types of tundra was developed. The geographic distributions of vegetation types north of 55°N, including the position of the forest limit and the distributions of the tundra types, could be predicted from climatology using a small set of plant functional types embedded in the biogeochemistry-biogeography model BIOME4. Several palaeoclimate simulations for the last glacial maximum (LGM) and mid-Holocene were used to explore the possibility of simulating past vegetation patterns, which are independently known based on pollen data. The broad outlines of observed changes in vegetation were captured. LGM simulations showed the major reduction of forest, the great extension of graminoid and forb tundra, and the restriction of low- and high-shrub tundra (although not all models produced sufficiently dry conditions to mimic the full observed change). Mid-Holocene simulations reproduced the contrast between northward forest extension in western and central Siberia and stability of the forest limit in Beringia. Projection of the effect of a continued exponential increase in atmospheric CO_2 concentration, based on a transient ocean-atmosphere simulation including sulfate aerosol effects, suggests a potential for larger changes in Arctic ecosystems during the 21st century than have occurred between mid-Holocene and present. Simulated physiological effects of the CO_2 increase (to >700 ppm) at high latitudes were slight compared with the effects of the change in climate. *INDEX TERMS:* 0315 Atmospheric Composition and Structure: Biosphere/atmosphere interactions; 1615 Global Change: Biogeochemical processes (4805); 1620 Global Change: Climate dynamics (3309); 1851 Hydrology: Plant ecology; *KEYWORDS:* tundra, biome, vegetation modeling, biogeography, ice age, mammoths

Citation: Kaplan, J. O., et al., Climate change and Arctic ecosystems: 2. Modeling, paleodata-model comparisons, and future projections, *J. Geophys. Res.*, *108*(D19), 8171, doi:10.1029/2002JD002559, 2003.

[1]Max Planck Institute for Biogeochemistry, Jena, Germany.
[2]Also at Plant Ecology, Department of Ecology, Lund University, Lund, Sweden.
[3]Now at Canadian Centre for Climate Modeling and Analysis, Victoria, British Columbia, Canada.
[4]Alaska Quaternary Center, University of Alaska, Fairbanks, Alaska, USA.
[5]Dynamic Paleoclimatology, Lund University, Lund, Sweden.
[6]Department of Geography, University of Oregon, Eugene, Oregon, USA.
[7]Climate Impacts Group, Department of Ecology, Lund University, Lund, Sweden.
[8]Now at Department of Physical Geography and Ecosystems Analysis, Lund University, Lund, Sweden.
[9]Potsdam Institute for Climate Impact Research, Potsdam, Germany.
[10]Department of Vegetation of the Far North, Komarov Botanical Institute, St. Petersburg, Russia.
[11]U.S. Geological Survey, Alaska Cooperative Fish and Wildlife Research Unit, University of Alaska, Fairbanks, Alaska, USA.
[12]University of Alaska Museum, Fairbanks, Alaska, USA.
[13]Institute of Arctic and Alpine Research, University of Colorado, Boulder, Colorado, USA.
[14]Institute of Arctic Biology, University of Alaska, Fairbanks, Alaska, USA.
[15]Quaternary Research Center, University of Washington, Seattle, Washington, USA.
[16]Alfred Wegner Institute for Polar and Marine Research, Forschungsstelle Potsdam, Potsdam, Germany.
[17]College of Forest Resources, University of Washington, Seattle, Washington, USA.
[18]Department of Geography, Norges Teknisk-Naturvitenskapelige Universitet, Trondheim, Norway.
[19]Now at Department of Geography, University of Southampton, Southampton, UK.
[20]Northeast Interdisciplinary Scientific Research Institute, Russian Academy of Sciences, Magadan, Russia.

Copyright 2003 by the American Geophysical Union.
0148-0227/03/2002JD002559$09.00

1. Introduction

[2] High-latitude ecosystems play a significant role in the global energy balance and carbon budget [*Oechel et al.*, 1993; *Foley et al.*, 1994; *Bonan*, 1995; *Chapin et al.*, 1996; *Christensen et al.*, 1999; *Chapin et al.*, 2000]. They have been simplistically treated in global modeling and global analyses of paleodata, which have commonly lumped them as a single biome, ''tundra,'' despite large variations in their physical and biogeochemical characteristics. In order to overcome some of the limitations of current treatments of tundra vegetation types, the Pan-Arctic Initiative (PAIN) has taken a comprehensive approach to describing and modeling terrestrial ecosystems of the northern high latitudes. The philosophy of PAIN has been to develop a model based on modern understanding and observations, and then to test the model at key times in the past where validation against paleodata is possible. We present a new, standardized classification of Arctic vegetation at the biome level, which may be identified floristically in the field and in pollen records, and simulated using a global vegetation model. We apply the model to the present day, Last Glacial Maximum (LGM, 21,000 years BP), the mid-Holocene (6000 years BP), and the end of the 21st century in a scenario with unchecked atmospheric CO_2 concentration increase. We compare the modeled vegetation to a map of present-day potential vegetation distribution, and to paleovegetation distributions inferred from pollen data. The future scenario allows us then to assess the sensitivity of Arctic vegetation to anthropogenic change in atmospheric CO_2 concentration and climate. The work is exploratory and makes use of existing results from several different general circulation models, according to availability. Nevertheless, we are able to draw some preliminary conclusions about the causes of observed vegetation changes in the Arctic, and about the sensitivity of high-latitude ecosystems to climate change.

2. Methods

2.1. Classification of Tundra Vegetation Types

[3] Most previous classifications of tundra vegetation types have been based on species assemblages and tailored to specific regions. Application of these schemes outside the region for which they were designed can be problematic. Widely used but loosely defined terms, such as ''high Arctic,'' ''subarctic,'' and ''polar desert'' have geographical connotations, which cause confusion, especially when applied to radically different environmental conditions in the past. We have therefore defined a new classification scheme for tundra vegetation types at the biome level. Each biome is defined in terms of physical structure and dominant life forms. We required that each biome also be floristically distinguishable, both in modern vegetation and in pollen-based reconstructions of paleovegetation. Given that species-level recognition of pollen is not often possible, the requirement that a biome can be reconstructed from pollen data is a strong constraint. However, it greatly increases the usefulness of the classification system by allowing modern and paleo-observations to be analyzed in a compatible way. Finally, we required that each biome occupy a unique and definable bioclimate space.

[4] Our scheme (Table 1; Figure 1) distinguishes five tundra biomes: low- and high-shrub; erect dwarf-shrub; prostrate dwarf-shrub; cushion forb, lichen, and moss; and graminoid and forb. Although it is possible to distinguish low-shrub and high-shrub tundra on physical grounds, it is not possible to distinguish these two vegetation types floristically and we therefore do not attempt to do so.

[5] Figure 1 was developed initially as a topology, based on our field experience. Quantitative expressions of the boundaries between biomes were developed empirically through the process of model development. The tundra biomes form a sequence along the gradient of accumulated growing-season temperature (expressed here as growing degree days above 0°C: GDD_0). The various forms of shrub-tundra are replaced by graminoid and forb tundra in dry habitats, especially areas that are regularly denuded of snow. Graminoid and forb tundra occurs with progressively higher levels of soil moisture as the growing-season temperature sum decreases. Figure 1 also shows the bioclimatic relationship between the tundra biomes and other high-latitude to midlatitude biomes: boreal and temperate forests, temperate grassland, and temperate xerophytic shrubland. The limits of temperate grassland and xerophytic shrubland are expressed in terms of soil moisture and GDD criteria. The boundary between tundra and boreal forests is expressed as a function of net primary productivity (NPP). Under modern climate conditions in the Arctic, forest NPP is highly correlated with GDD [*Gower et al.*, 1997; *Schulze et al.*, 1999]. However, the definition of this limit in terms of NPP is somewhat more mechanistic as it reflects the requirement for a minimum carbon balance to sustain the growth and reproduction of trees. Furthermore, the use of NPP as a limit on tree growth may provide a more realistic way of simulating tree line in the past under lowered atmospheric CO_2 concentration ($[CO_2]_{atm}$) [*Walter*, 1973; *Tranquillini*, 1979; *MacDonald and Gajewski*, 1992; *Jolly and Haxeltine*, 1997; *Street-Perrott et al.*, 1997; *Cowling*, 1999; *Körner*, 1999].

2.2. BIOME4 Model

[6] BIOME4 was developed from the BIOME3 model of *Haxeltine and Prentice* [1996a]. BIOME4 is a coupled carbon and water flux model that predicts global steady state vegetation distribution, structure, and biogeochemistry, taking account of interactions among these aspects. The model is driven by long-term averages of monthly mean temperature, sunshine and precipitation. In addition, the model requires information on soil texture and soil depth in order to determine water holding capacity and percolation rates. $[CO_2]_{atm}$ is specified.

[7] Twelve plant functional types (PFTs) in BIOME4 represent broad, physiologically distinct classes, ranging from cushion forbs to tropical rain forest trees [*Kaplan*, 2001]. Each PFT is assigned a small number of bioclimatic limits which determine whether it could be present in a given grid cell, and therefore whether its potential net primary productivity (NPP) is calculated; and a set of parameter values which define its carbon and water exchange characteristics. The computational core of BIOME4 is a coupled carbon and water flux scheme, which determines the seasonal maximum leaf area index (LAI) that maximizes NPP for any given PFT, based on a daily time step simulation of soil water balance and monthly process-

Table 1. Circumpolar Tundra Biome Classification

Biome	Definition	Typical Taxa
Low- and high-shrub tundra	continuous shrubland, 50 cm to 2 m tall, deciduous or evergreen, sometimes with tussock-forming graminoids and true mosses, bog mosses and lichens	*Alnus*, *Betula*, *Salix*, *Pinus pumila* (in eastern Siberia), *Eriophorum*, *Sphagnum*
Erect dwarf-shrub tundra	continuous shrubland 2–50 cm tall, deciduous or evergreen, with graminoids, true mosses and lichens	*Betula*, *Cassiope*, *Empetrum*, *Salix*, *Vaccinium*, Gramineae, Cyperaceae
Prostrate dwarf-shrub tundra	discontinuous shrubland of prostrate deciduous shrubs, 0–2 cm tall	*Salix,Dryas*, *Pedicularis*, Asteraceae, Caryophyllaceae, Gramineae, true mosses
Cushion forb, lichen and moss tundra	discontinuous cover of rosette plants or cushion forbs with lichens and mosses	*Papaver, Draba*, Saxifragaceae, Caryophyllaceae, lichens, true mosses
Graminoid and forb tundra	predominantly herbaceous vegetation dominated by forbs and graminoids, with true mosses and lichens	*Artemisia, Kobresia*, Brassicaceae, Asteraceae, Caryophyllaceae, Gramineae, true mosses

based calculations of canopy conductance, photosynthesis, respiration and phenological state [*Haxeltine and Prentice*, 1996a]. The model is sensitive to CO_2 concentration because of the responses of NPP and stomatal conductance to CO_2 and the differential effects of CO_2 on the NPP of C_3 and C_4 plants.

[8] To identify the biome for a given grid cell, the model ranks the tree and nontree PFTs that were calculated for that grid cell. The ranking is defined according to a set of rules based on the computed biogeochemical variables, which include NPP, LAI, and mean annual soil moisture. The resulting ranked combinations of PFTs lead to an assignment to one of 27 biomes.

2.3. High-Latitude PFTS and Biomes in BIOME4

[9] High-latitude biomes are represented in BIOME4 by combinations of a restricted set of frost-tolerant PFTs. Several have been recognized and used in earlier versions of the BIOME model (e.g., cold deciduous tree, cold needleleaf evergreen tree). Three PFTs (cold shrub, cold graminoid or forb, and cushion forb) used to distinguish the tundra biomes have been newly defined for BIOME4. Each of these tundra PFTs was assigned values of required model parameters (Table 2) based on available physiological information [see, e.g., *Ehleringer and Björkman*, 1977; *Berry and Björkman*, 1980; *Berry and Downton*, 1982; *Farquhar and von Caemmerer*, 1982; *Kirschbaum and Farquhar*, 1984; *Larcher*, 1995, *Körner*, 1999] with supplementary limits inferred by comparison of species distributions with climate data. These three new tundra PFTs use the C_3 photosynthetic pathway, are shallow rooting, and are susceptible to water stress and fire.

[10] The nontundra PFTs used by BIOME4 to simulate high-latitude vegetation types include cold and temperate broadleaf and needleleaf trees, xerophytic shrubs, and temperate grasses. These PFTs are also defined by a set of bioclimatic limits and physiological parameters [*Kaplan*, 2001]. Where tree PFTs satisfy bioclimatic limits and NPP and soil moisture requirements, they always dominate over grasses and shrubs. Temperate xerophytic shrub and temperate grass PFTs may use both the C_3 and C_4 photosynthetic pathways; carbon gain is optimized for the pathway on a seasonal basis for grasses. All tree PFTs use C_3 photosynthesis. Other physiological parameters that vary among the

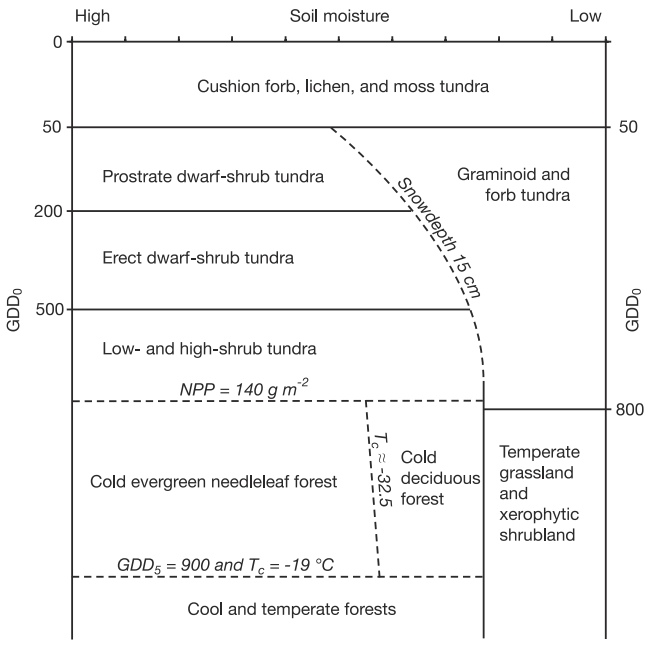

Figure 1. Climate space occupied by northern high-latitude biomes.

Table 2. Distinctive Bioclimatic Limits and Physiological Parameters for Tundra PFTs[a]

	Cold Shrub	Cold Graminoid or Forb	Cushion Forb
Bioclimatic Limits			
Minimum GDD_0, °C	50	50	
Minimum snow depth, cm	15		
Physiological Parameters			
Phenology	evergreen	summergreen	evergreen
GDD_0, °C		25	
R_s	yes	no	yes
Optratio	0.9	0.75	0.8
kk	0.5	0.3	0.6
T_{pC3} (°C)	−7	−7	−12
T_{curve}	0.6	0.6	0.5
Alloc	1	1	1.5

[a]GDD_0, sum of GDD_0 required to grow a full canopy; R_S, presence of sapwood respiration; optratio, maximum ratio of leaf-internal to ambient partial pressure of CO_2; kk, the Beer's law extinction coefficient; T_{pC3}, minimum mean monthly temperature for photosynthesis; T_{curve}, parameter of the response of photosynthesis to temperature; Alloc, modifier to the minimum allocation.

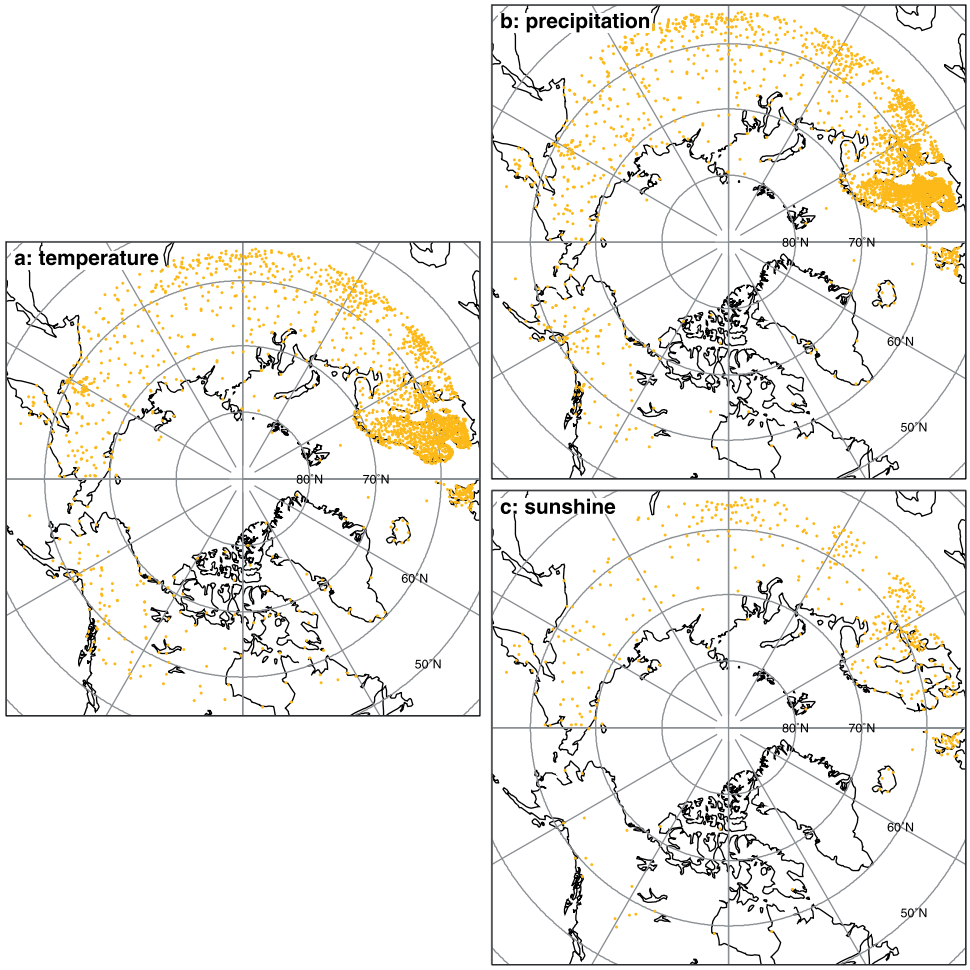

Figure 2. Distribution of sites north of 55 °N with monthly means of (a) temperature, (b) precipitation, and (c) fractional sunshine hours in the CLIMATE 2.2 data set.

tree PFTs are canopy architecture, root depth distribution, transpiration characteristics, phenology, leaf habit, and the responses of photosynthesis and respiration to temperature.

[11] Biomes are assigned based on a set of rules that uses the dominant PFT, in some cases the sub-dominant PFTs (ranked according to simulated values of NPP, LAI, and mean annual soil moisture), and certain environmental limits (Figure 1). Thus there is no simple correspondence between the presence/absence of PFTs and the assignment of biomes. This is an important conceptual difference between the modeling approach described here and the approach of reconstructing biomes from pollen data [e.g., *Bigelow et al.*, 2003], in which the complete set of available floristic information is used to diagnose the biome.

2.4. Climate Scenarios

2.4.1. Baseline Climatology

[12] We used a gridded long-term mean climatology (temperature, precipitation, sunshine) for the late 20th century (CLIMATE 2.2) see (http://www.pik-potsdam.de/~cramer/climate.htm) for the modern vegetation simulation, and as the baseline for the other modeling experiments. Version 2.2 of CLIMATE includes more station data from sparsely populated regions and particularly the Arctic, compared to earlier versions of the dataset, and an improved estimation of the elevational gradients of climate variables. The station coverage for the high northern latitudes is shown in Figure 2. The gridded dataset was generated by interpolating long-term station mean values for monthly temperatures, monthly percentages of potential sunshine hours, and monthly total precipitation. Three-dimensional interpolation of the 36 climate variables was performed using the method of thin-plate smoothing splines [*Hutchinson and Bischof*, 1983; *Hutchinson*, 1995]. This method is highly appropriate for interpolating climate data from a sparse or irregular network of stations, and has been shown to minimize errors in areas of complex terrain [*Price et al.*, 2000].

[13] The smoothing spline method yields smooth functions of longitude, latitude and elevation. These functions were evaluated at the model elevation of each grid cell of a 0.5° geographic grid [*Geophysical Exploration Technology* (*GETECH*), 1996]. The evaluations were made at all land grid cells north of 55°N, including "virtual" land grid cells on the continental-shelf areas that were exposed at the LGM. The LGM land mask was derived by tracing the −125 m contour [*Fleming et al.*, 1998] on modern bathymetry [*GETECH*, 1996].

[14] An atmospheric CO_2 concentration of 324 ppm was used to force BIOME4 for the present-day baseline simulation. This is approximately the mean $[CO_2]_{atm}$ during the

period of measurement of the climate station data used in CLIMATE 2.2.

2.4.2. Paleoclimate Simulations

[15] BIOME4 simulations were made for the LGM (~21,000 years BP) and mid-Holocene (~6000 years BP). These two periods have been a major focus for paleoclimate modeling [e.g., *Joussaume and Taylor*, 1995, 2000; *Kohfeld and Harrison*, 2000] because they represent extremes of climate forcing. At the LGM, the Earth's orbital configuration was similar to today but greenhouse gas concentrations were low [*Raynaud et al.*, 1993], Northern Hemisphere ice sheets were greatly expanded [*Denton and Hughes*, 1981] and sea level was low [*Fairbanks*, 1989]. In addition to the large changes in terrestrial geography, the ocean surface was colder and the distribution of sea ice was expanded [*CLIMAP*, 1981]. The configuration of the Earth's orbit was substantially different from today or the LGM during the intervening period of the early to mid-Holocene. The phasing of the precession (19, 23 ka) and obliquity (41 ka) cycles was such that the high latitudes of the Northern Hemisphere received a maximum in insolation, both during boreal summer and annually, at ~11,000 calendar years bp. This anomaly decayed gradually toward the present. As a direct radiative effect of the orbital forcing, many regions of the Arctic experienced early Holocene summers that were considerably warmer than present [see, e.g., *Ritchie et al.*, 1983; *Bradley*, 2000; *MacDonald et al.*, 2000]. But the Laurentide ice sheet, although substantially reduced from the LGM, was still sufficiently large to have a major downwind cooling effect during the early Holocene [*Mitchell et al.*, 1988; *Harrison et al.*, 1992]. Northern Europe and eastern North America therefore experienced a thermal maximum several thousand years after the insolation maximum [*Wright et al.*, 1993]. For this reason, investigations of the impact of insolation changes on climate have conventionally focused on 6000 years BP, when the difference in orbital configuration was still large but the impact of the small residual Laurentide ice sheet was restricted.

[16] Several atmospheric general circulation models (AGCMs) have performed simulations of the LGM using a standard protocol [*Joussaume and Taylor*, 1995, 2000]. In this protocol, orbital parameters are set for 21,000 calendar years bp [*Berger*, 1978], the extent and height of the ice sheets are prescribed from *Peltier* [1994], land-sea distribution, sea-surface temperatures and the seasonally varying distribution of sea ice are prescribed from *CLIMAP* [1981], and $[CO_2]_{atm}$ is set to 200/345 of the value used in the model's control simulation. New paleoceanographic data suggest that the CLIMAP representation of the LGM ocean is incorrect for some regions. Seasonal changes in SSTs and sea-ice extent in the North Atlantic were probably greater than shown by CLIMAP [*Sarnthein et al.*, 1995; *de Vernal and Hillaire-Marcel*, 2000] while the tropical ocean surface was generally cooler than shown by CLIMAP [*Mix et al.*, 1986; *Rosell-Melé et al.*, 1998; *Hostetler and Mix*, 1999]. Comparisons of simulations and paleoenvironmental data from the tropics suggests that some simulations made with computed (mixed-layer ocean) SSTs may be more realistic than those driven by CLIMAP SSTs [*Pinot et al.*, 1999]. However, the mixed-layer ocean simulations studied by *Pinot et al.* [1999] differed greatly from one another, and none captured the observed spatial patterning in tropical cooling on land [*Farrera et al.*, 1999]. There has been no systematic analysis of the performance of mixed-layer ocean simulations of the LGM in the high latitudes. We have therefore adopted CLIMAP-driven simulations, while recognizing that they may not be entirely realistic. We chose four simulations for the LGM among those studied by *Pinot et al.* [1999] in order to encompass the range of simulated high-latitude climates (especially simulated summer temperature and precipitation changes). We used simulations performed with two versions of the Laboratoire de Météorologie Dynamique (LMD) model (LMD4, LMDH) [*Le Treut et al.*, 1994; *Masson et al.*, 1998; *Ramstein et al.*, 1998], the Meteorological Research Institute, Japan AGCM-IIb model (MRI2) [*Kitoh et al.*, 1995], and the UK Universities' Global Atmospheric Modeling Programme model (UGAMP) [*Dong and Valdes*, 1998]. Among these simulations for the northern high latitudes, LMD4 represents a "wet" end-member and LMDH is a "dry" end-member in terms of annual precipitation anomalies. MRI2 and UGAMP are "warm" and "cold" end-members, respectively, in terms of summer (JJA) temperature anomalies.

[17] Ocean feedbacks had a significant impact on mid-Holocene climates, both in the tropics and at high-latitudes [*Kutzbach and Liu*, 1997; *Texier et al.*, 1997; *Braconnot et al.*, 1999; *Harrison et al.*, 2003]. We therefore did not use mid-Holocene simulations that assumed unchanged (modern) SSTs, as by, e.g., *Texier et al.* [1997]. Simulations of the 6000 years bp climate have more recently been performed by several coupled ocean-atmosphere general circulation models (OAGCMs) [*Hewitt and Mitchell*, 1998; *Otto-Bliesner*, 1999; *Braconnot et al.*, 2000, 2003]. We used output from version 2 of the Hadley Centre coupled model (HADCM2) [*Hewitt and Mitchell*, 1998], and the Institut Pierre Simon Laplace coupled model (IPSL-CM1) [*Braconnot et al.*, 2000] as illustrative simulations of the mid-Holocene climate. Both simulations were forced only by orbital changes; CO_2 concentration, ice sheets and land-sea geography were unchanged from the control simulations of each model.

[18] Paleoclimate scenarios for the LGM and mid-Holocene were derived from the climate model outputs by an anomaly procedure; i.e., subtracting the control climate simulation of each GCM from the palaeo simulation of that model, and adding the resulting "anomaly" (with suitable interpolation) to the present-day baseline climatology. The anomaly approach compensates for first-order bias in the model control simulations. However, we cannot rule out the possibility that biases in a model also affect the sensitivity of that model to boundary condition changes [*de Noblet-Ducoudré et al.*, 2000; *Braconnot et al.*, 2002]. In generating the LGM climatologies, we made a small correction of temperature to account for the topographic difference between the LGM land surface as modeled by *Peltier* [1994] and the simplified topography used in the model, using a standard lapse rate.

[19] CO_2 concentrations for BIOME4 simulations were prescribed as follows: (1) for "modern" conditions, 324 ppm; (2) for mid-Holocene, 324 ppm (i.e., unchanged from modern, for consistency with the OAGCM simulations); (3) for LGM, 188 ppm (= 200/345 * 324 ppm, i.e., reduced by the same factor as in the AGCM simulations).

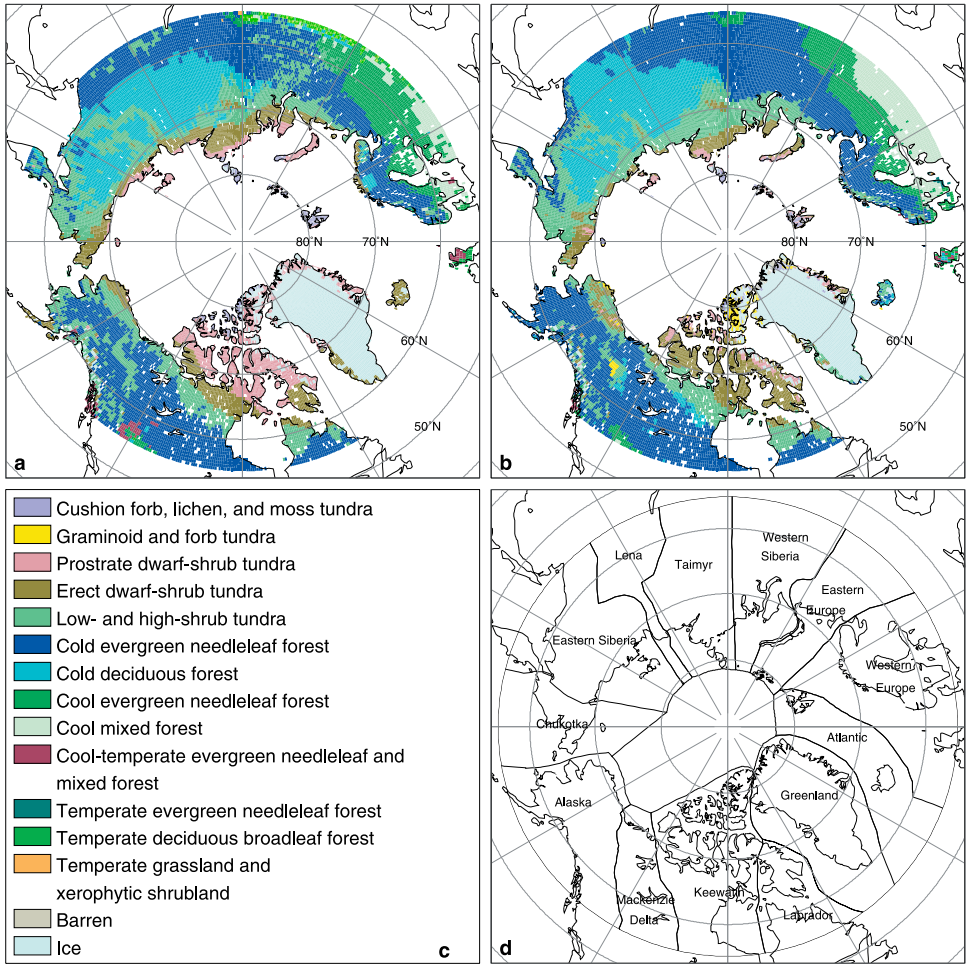

Figure 3. Present-day (a) potential natural vegetation and (b) vegetation simulated by BIOME4 north of 55° N, with legend (c). The map (d) delineates the sectors used in Table 4 and in the text.

2.4.3. Future Projection

[20] To assess the sensitivity of Arctic vegetation to possible future climate changes we again used results from the HADCM2 model forced by the IS92a greenhouse gas and sulphate aerosol concentration scenario for the 21st century [*Hulme et al.*, 1999]. We used the mean climate anomalies from the final ten years of the simulation (2090–2100). $[CO_2]_{atm}$ for BIOME4 was prescribed to increase by the same factor as in the OAGCM. We also performed a sensitivity test with $[CO_2]_{atm}$ unchanged at 324 ppm. The same OAGCM scenario has been applied in several studies on the sensitivity of vegetation to future climate change [*Neilson et al.*, 1998; *Malcolm and Markham*, 2000; *Cramer et al.*, 2001]. The simulation is not intended as a realistic forward projection and it does not include the potentially significant feedbacks between land-surface and atmosphere. It is used here simply to illustrate a possible course of the climate change and thus to give an impression of the sensitivity of Arctic ecosystems to the climate changes that might be induced by increasing greenhouse gas concentrations if these continue to increase at their present rate.

2.5. Earth Surface Properties

[21] As input to BIOME4, we used the land area and derived soil properties defined in the FAO digital soil map of the world [*Food and Agriculture Organization*, 1995] to create a data set on soil water holding capacity and percolation rate for the present day, mid-Holocene and "future" simulations. For the LGM simulations we used the present-day soils dataset as a baseline and overlaid information on ice sheets [*Peltier*, 1994; *Svendsen et al.*, 1999], sea level [*Fleming et al.*, 1998], and lakes and inland seas [*Kvasov*, 1979, 1975; *Dyke and Prest*, 1987].

2.6. Validation Data Sets

[22] A provisional map of present-day potential natural vegetation north of 55° N (Figure 3a) was produced by combining information from two sources. Tundra vegetation distributions are based on the preliminary field-based mapping by *Walker* [2000]. The distribution of other vegetation types and the location of the forest limit were derived from the composite potential natural vegetation map of *Haxeltine and Prentice* [1996a], with minor modifications of nomenclature. The reliability of the resulting map is unknown, and could only be (ultimately) assessed by remote sensing approaches that are still under development. We consider the sources behind this map as the best currently available, and we emphasize that it does not contain any assumed bioclimatic relationships or model. It has also been shown to be broadly consistent with surface

pollen data [*Bigelow et al.*, 2003]. Pollen data from lake and mire sediments represent vegetation in a 10–30 km region around the sampling locations [*Jacobson and Bradshaw*, 1981; *Prentice*, 1988; *Sugita et al.*, 1998] and therefore can give an acceptable representation of large-scale vegetation patterns [*Webb et al.*, 1978; *Prentice et al.*, 1996; *Guiot et al.*, 1996], today and in the past.

[23] Maps of vegetation at the LGM (defined for data compilation as 18,000 ± 1000 ^{14}C years BP, approximately equivalent to 21,000 calendar years BP) and mid-Holocene (defined as 6000 ± 500 ^{14}C years BP) have been produced based on pollen data from the region north of 55°N [*Bigelow et al.*, 2003] using a standard procedure (known as biomization; see *Prentice et al.* [1996]) and the classification scheme for tundra and boreal biomes used in BIOME4 (Figure 1; Table 1). The sampling locations, age models used for the selection of samples, allocation of pollen taxa to PFTs, and the allocation of PFTs to biomes are described in detail by *Bigelow et al.* [2003].

3. Results

3.1. Present Day

[24] In a quantitative comparison between the simulated vegetation map (Figure 3b) and the modern potential vegetation map (Figure 3a), 60.4% of grid cells (16,111 cells, excluding ice-covered cells) showed the same biome. Percentage agreement for grid cells assigned to specific forest biomes in the potential vegetation map were: temperate deciduous broadleaf forest 35.3%; cool mixed forest 78.2%; cool evergreen needle-leaved forest 72.1%; cool-temperate evergreen needleleaf and mixed forest 14.4%; cool evergreen needleleaf forest 87.2%; cold deciduous forest 73.0%. For tundra biomes the figures were: low- and high-shrub tundra 50.4%; erect dwarf-shrub tundra 37.5%; prostrate dwarf-shrub tundra 17.0%; cushion forb, lichen, and moss tundra 42.2%. The most important mismatches (where >20% of cells assigned to one biome in the potential vegetation map were assigned to a different biome in the simulation) were between adjacent biomes in climate space (Figure 1): temperate deciduous broadleaf forest, cool mixed forest, 49.4%; cool evergreen needle forest, cool mixed forest, 27.1%; cool-temperate evergreen needleleaf and mixed forest, cool (20.2%) or cold (42.3%) evergreen needleleaf forest; low- and high-shrub tundra, cold evergreen needleleaf forest, 32.4%; erect dwarf-shrub tundra, low- and high-shrub tundra, 53.8%; prostrate dwarf-shrub tundra, erect dwarf shrub-tundra, 53.6%; cushion-forb, lichen, and moss tundra, prostrate dwarf-shrub tundra, 34.6%. The apparently large error in the simulated area of temperate deciduous forest is due to a discrepancy in the placement of the temperate deciduous tree limit in eastern Europe. This is a slight difference compared with the total distribution of temperate deciduous forest, which lies mainly south of 55°N. The area of cool-temperate evergreen needleleaf and mixed forest north of 55°N is restricted and the simulation misses its occurrence in the prairie-forest transition region of Canada.

[25] For nonforest biomes, the largest differences between the potential vegetation map and the simulation are due to a discrepancy in the location of the boundary between the two dwarf-shrub tundra biomes in Keewatin. The potential vegetation map places this boundary further south than the simulation, apparently at a higher GDD level (according to the climate data) than the same boundary in Siberia. The boundary between low- and high-shrub tundra and erect dwarf-shrub tundra is also placed somewhat too far north by the simulations. Graminoid and forb tundra is not shown in the potential vegetation map but it occurs locally in suitable habitats throughout drier parts of the Arctic [*Edwards and Armbruster*, 1989; *Lloyd et al.*, 1994; *Young*, 1976; *Yurtsev*, 1982], usually in topographic locations that are regularly denuded of snow. The simulated distribution of this biome north of 55°N is restricted to dry climates in the Mackenzie Delta region, Keewatin (Ellesmere Island) and northern Greenland. Altogether 21.3% of nonforest cells were simulated as forest (19.0% due to low- and high-shrub tundra cells being simulated as the treeline-forming biomes, cold needleleaf evergreen or cold deciduous forest), and 6.4% of forest cells were simulated as nonforest (6.1% due to the opposite misclassification, i.e., low- and high-shrub tundra cells simulated as cold needleleaf evergreen or cold deciduous forest). The difference between these figures indicates a bias toward the simulation of forest. Tundra is more extensive in southern and western Alaska than the model indicates, and in western Siberia some wetland areas appear to have been classified as tundra in the potential vegetation map. These two differences are the main cause of the bias; no bias is apparent in the simulated geographic position of the northern forest limit (Figure 3b).

[26] Simulated NPP in the tundra biomes ranged from >200 g C m^{-2} years^{-1}, for high and low shrubs, to <70 g C m^{-2} years^{-1} for cushion forbs (Table 3). The ranges for simulated productivity are similar to those measured in the field, though particularly favorable micro-site conditions may explain measured higher productivity values (>300 g C m^{-2} years^{-1}) in small areas [*Christensen et al.*, 2000; *Shaver and Chapin*, 1991].

3.2. Last Glacial Maximum

[27] Major changes in vegetation cover at the LGM compared to present are shown by all four LGM simulations (Figure 4). The simulated tundra vegetation was considerably more extensive than today and simulated forests were confined to the southernmost part of the region, in eastern Europe and western Siberia. The majority of the simulations also indicate a limited area of forest on the Bering land bridge. The available palaeovegetation data (Figure 4e) are too sparse to allow quantitative comparison with the simulations, but they support the simulation of continuous tundra across the unglaciated regions of Eurasia and North America. Vegetation reconstructions from southern Europe [*Elenga et al.*, 2000] and further south in Russia [*Tarasov et al.*, 2000] also indicate nonforest (tundra or grassland) vegetation at the LGM. Thus even the limited presence of forests in Eurasia north of 55°N as indicated by the simulations is probably an overestimate. Evaluations of the LGM simulations discussed by *Pinot et al.* [1999], including the four models presented here, suggest that the models generally do not produce a sufficiently large cooling in the mid- to high-latitudes, compared to paleoenvironmental observations [*Kageyama et al.*, 2001]. This finding is consistent with underprediction of the area of tundra at the LGM.

Table 3. Average and Standard Deviation of NPP for Tundra Biomes in the Present-Day Simulation

BIOME	NPP, g C m^{-2} $years^{-1}$
Low- and high-shrub tundra	223 ± 44
Erect dwarf-shrub tundra	160 ± 28
Prostrate dwarf-shrub tundra	99 ± 23
Cushion forb, lichen and moss tundra	71 ± 37
Graminoid and forb tundra	85 ± 55

[28] The pollen data show that low- and high-shrub tundra was greatly reduced in extent at the LGM while graminoid and forb tundra was extensive [*Bigelow et al.*, 2003]. These features are simulated, although to different extents by the different models. LMDH best approximates the reconstructed distribution of this biome, and shows quantitatively the best overall agreement with the palaeodata. The extent of graminoid and forb tundra simulated by

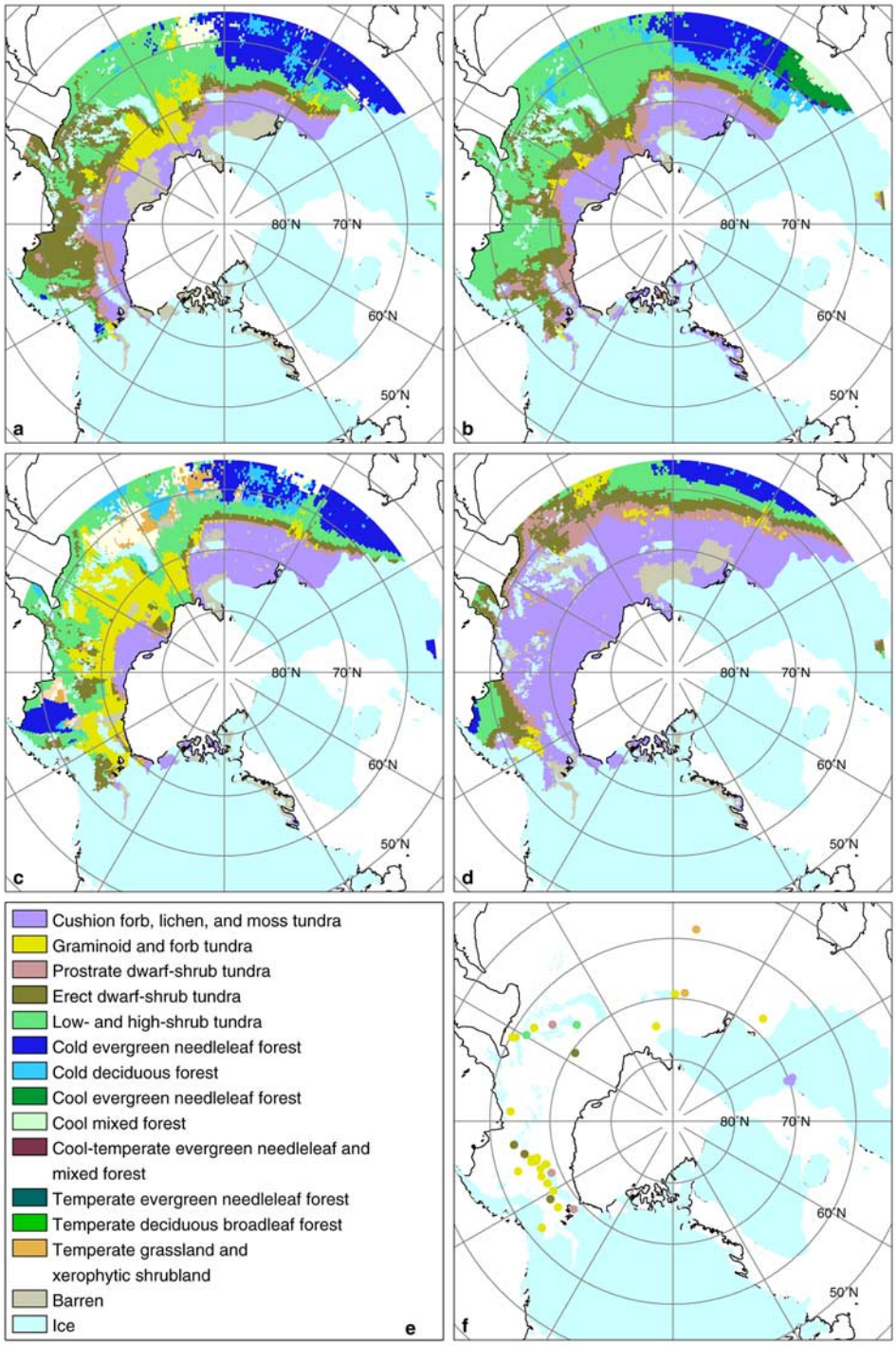

Figure 4. LGM vegetation patterns simulated by BIOME4 driven by output from four atmospheric general circulation models, (a) MRI2, (b) LMD4, (c) LMDH, and (d) UGAMP, compared to (f) observed vegetation reconstructed from pollen data [*Bigelow et al.*, 2003].

MRI2 also approximates the observed distribution in western and central Siberia, although low temperatures in eastern Siberia in MRI2 result in the simulation of cushion forb, lichen, and moss tundra over too large an area. The expansion of graminoid and forb tundra in the LMD4 simulation is very small and does extend outside the Arctic. Again, cushion forb, lichen and moss tundra is simulated over too large an area. The simulated expansion of cushion forb, lichen, and moss tundra, which is most pronounced in the BIOME4 simulation using the UGAMP anomaly climatology but is shown in all of the simulations, is hard to evaluate from paleodata. One ice-marginal location (Andøya, in NW Norway) is characterized as cushion forb, lichen, and moss tundra in the LGM paleovegetation reconstruction (Figure 4e) [*Bigelow et al.*, 2003]. The core areas of the simulated expansion of cushion forb, lichen, and moss tundra (along the northern Siberian coast and along the eastern margin of the European ice sheet) are not represented in the palaeodata, probably because the extreme conditions which favor this biome are often unfavorable for sedimentation and pollen preservation.

3.3. Mid-Holocene

[29] The two mid-Holocene simulations agree in showing relatively small vegetation changes in comparison to the present. (Figures 5a and 5b). Northward displacements of the forest limit were quantified (Table 4) from the palaeodata and from the simulations, by plotting the mean percentage of forested data points (or grid cells) in each sector as a function of latitude, estimating the latitude corresponding to 50% forest cover, and differencing the mid-Holocene and present-day estimates. Both simulations indicate modest northward shifts of the forest limit (50–100 km) in western/central Siberia and in Labrador and Keewatin, and little or no change elsewhere. The pollen data show northward shifts of 50–150 km in central Siberia, and 50–100 km in western Europe and the Mackenzie Delta region. The data also indicate that the treeline was further south than present in Keewatin and Labrador. The data are insufficient to yield reliable estimates for all regions (Table 4) but they indicate a clear divergence of sign from the simulations in eastern Canada. Otherwise, the models and data agree on the sign and the order of magnitude of the shift, and on its asymmetry around the pole: the more northerly location of the polar forest limit in western or central Siberia contrasts with no change in eastern Siberia, Chukotka, and Alaska. This asymmetry is a robust feature of the data. It was shown (based on a limited set of observations) by *TEMPO Members* [1996], and is corroborated by independent reconstructions based on preserved tree stumps north of the present tree limit in Eurasia [*MacDonald et al.*, 2000]. The simulated northward shifts in tundra vegetation belts are also most pronounced in central Siberia and in Labrador/Keewatin while very little change in tundra vegetation is simulated in other Arctic regions. Observed changes in tundra vegetation belts support the idea that the largest changes occur in Labrador/Keewatin, and also in Greenland [*Bigelow et al.*, 2003]. There is insufficient data from central Siberia to determine how large the changes there were. There are no systematic shifts in tundra vegetation in other regions.

[30] Simulated changes in vegetation south of the tree line are more pronounced. In both simulations, the northern margin of cool evergreen needleleaf forest in Scandinavia and eastern Europe is 300–500 km north of its position in the modern simulation. The northern margin of cool mixed forest is displaced northward by 50–200 km. Large northward displacements of cool and temperate forest zones are also observed in North America, mainly south of 55°N. The paleovegetation data confirm that the northward shift of cool and temperate forests was larger than changes in the northern tree line in any sector. Indeed, the pollen data suggest that the simulated northward shifts (e.g., of temperate deciduous broadleaf forest in the European sector) were smaller than those that occurred.

[31] In the continental interior of Eurasia, the simulations show the appearance of temperate grasslands and xerophytic shrublands due to increased aridity. Expansion of drought-tolerant vegetation, including temperate grasslands and xerophytic shrublands, is also simulated in mid-continental North America. This prediction is realistic for North America [*Harrison et al.*, 2003]. However, the pollen-based reconstructions of mid-Holocene vegetation show no expansion of drought-tolerant biomes in the continental interior of Eurasia. This finding is consistent with earlier reconstructions based on pollen data [e.g., *Tarasov et al.*, 1998], and with independent evidence based on geomorphic and biostratigraphic records of changes in lake status that show little or no change in the regional water balance of central Eurasia in the mid-Holocene [*Harrison et al.*, 1996].

3.4. Future Sensitivity

[32] In the illustrative simulation of a "greenhouse climate," the potentially forested area of the Arctic increases substantially (Figure 5c). The simulated tree line is farther north than indicated by either the mid-Holocene simulations in most sectors (Table 4), unless expansion is precluded by the coastline. Trees are shown potentially invading coastal Greenland and Chukotka, where only fragments of forest exist today. The area of cold deciduous forest is strongly reduced. with replacement by evergreen forests, as also found by *Cramer et al.* [2001] with several dynamic global vegetation models. Thus the simulations indicate a much larger sensitivity of the forest limit to CO_2-induced warming than to the orbitally induced warming of the mid-Holocene. A sensitivity experiment with $[CO_2]_{atm}$ held constant (not shown) indicates that the simulated vegetation changes were almost entirely due to the simulated change in climate. Physiological effects of the CO_2 increase on the polar forest limit were negligible.

[33] The "greenhouse climate" simulation also indicates major northward shifts of the shrub-dominated tundra biomes and a further reduction in the areas occupied by cushion-forb, lichen, and moss tundra and by graminoid and forb tundra. These simulated changes are also larger than the changes in tundra vegetation shown in the simulations of the mid-Holocene.

4. Discussion

4.1. Present Day

[34] BIOME4 captures the main features of vegetation distribution in the northern high latitudes: the position of the

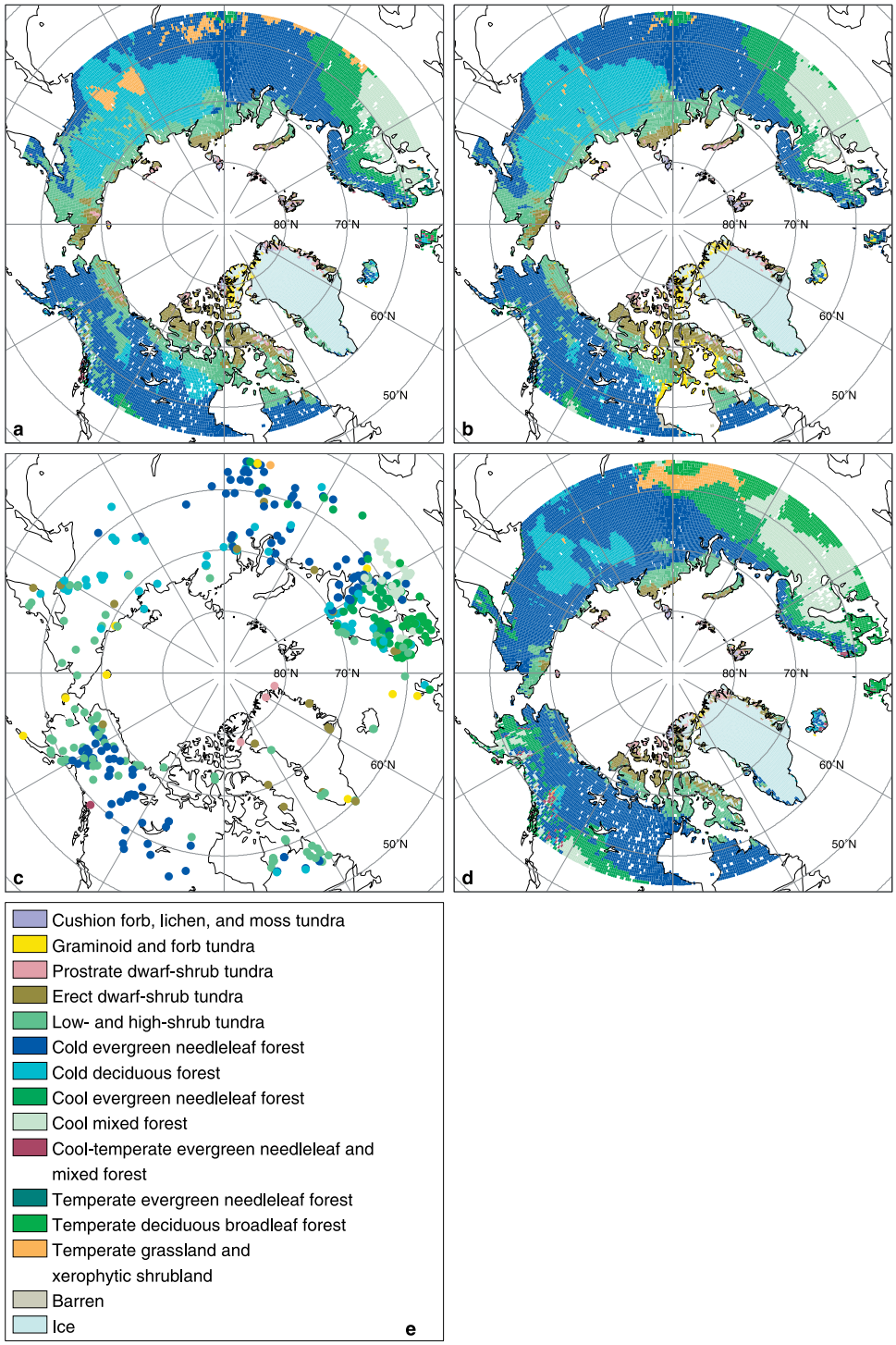

Figure 5. Mid-Holocene vegetation patterns simulated by BIOME4 driven by output from (a) the IPSL-CM1 and (b) the HADCM2 coupled ocean-atmosphere general circulation models, compared to (c) observed vegetation reconstructed from pollen data [*Bigelow et al.*, 2003]. The potential vegetation (d) driven by the mean climate of the decade 2090–2100 simulated by the HADCM2-SUL coupled model, using the IS92a scenario, is also shown.

northern forest limit, its composition in terms of evergreen versus deciduous trees, and the observed diversity and geographic extent of tundra vegetation types. Simulated estimates of tundra NPP are within the range of field measurements. In those hypermaritime tundra regions where the model incorrectly simulates forest (principally southwestern Alaska, but also some locations in northwestern Europe and Chukotka), the influence of heavy cloud cover combined with low sun angles on surface solar radiation may be responsible for the disagreement. Addi-

Table 4. Changes (Relative to Present) in the Latitude (°) of the Northern Forest Limit[a]

	Mid-Holocene		2090–2100	
Sector	Palaeodata[b]	HADCM2	IPSL-CM1	HADCM2-SUL
Alaska	no change	no change	no change	+1.5°
Mackenzie Delta	+0.5°	no change	−0.5°	+0.5°
Keewatin	−2.5°	+0.5°	+0.5°	+2.0°
Labrador	−1.5°	+0.5°	+0.5°	+1.5°
Greenland		no change	no change	+4.0°
Western Europe	+0.5°	no change	no change	+0.5°
Eastern Europe		no change	no change	+1.0°
Western Siberia		+0.5°	+0.5°	+1.5°
Taimyr	+1.5°	+1.0°	no change	+2.0°
Lena	+0.5°	no change	no change	+0.5°
Eastern Siberia	no change	no change	no change	+1.5°
Chukotka		no change	no change	+2.5°

[a]The sectors are defined in Figure 3.
[b]Estimates were made in cases where the pollen sites bracketed the forest limit both for the present (surface samples) and mid-Holocene. In other cases no well-founded estimate could be made and therefore this column is left blank.

tional sensitivity experiments (not shown) demonstrated that a reduction in incoming short-wave radiation by 25%, by reducing NPP, would lead to the simulation of low- and high-shrub tundra in these regions. Such a reduction, compared with the values simulated by the simple empirical cloud-radiation algorithm in BIOME4 [*Linacre*, 1968; *Prescott*, 1940], is plausible based on observations [*Henderson-Sellers*, 1986].

[35] The boundary between erect and prostrate dwarf-shrub tundra in the Canadian Arctic seems to be misplaced by the model. It is unlikely, however, that this boundary occurs at different GDD in Canada and Siberia. Resolution of this issue may require improved mapping of the vegetation boundaries, especially in the Canadian Arctic [*Walker*, 2000]. Gaps in the distribution of weather stations in some areas may be responsible for local artifacts in the simulation, notably in the northern coastal lowlands of Alaska [*Fleming et al.*, 2000].

4.2. Last Glacial Maximum

[36] Palaeodata support the simulated extension of tundra across present-day forest regions, the restriction of low- and high-shrub tundra, and the large expansion of graminoid and forb tundra at the LGM. But only one of the simulations (LMDH) produces an increase in graminoid and forb tundra of comparable magnitude to the observed expansion. The other simulations produce too much snowfall in Siberia and Beringia, leading to overprediction of the dwarf-shrub tundra biomes.

[37] The climate model results must be considered provisional because they assumed CLIMAP SSTs, they imposed an "East Siberian Ice Sheet" (not shown on the maps) which was not present at the LGM (probably leading to unrealistic circulation patterns, as well as local underestimation of temperature [*Felzer*, 2001], and they do not take account of vegetation feedbacks (although the physical land-surface conditions evidently changed drastically between LGM and present). Nevertheless, the results yield insight into the causes of LGM vegetation patterns. The LGM graminoid and forb tundra is of special interest because of its floristic diversity, and because it supported a high population density of large mammals, including mammoths [*Guthrie*, 2001]. The nature of this vegetation has been controversial [*Brubaker et al.*, 1983; *Guthrie*, 1985; *Ritchie*, 1985; *Guthrie and Stoker*, 1990; *Lloyd et al.*, 1994; *Zimov et al.*, 1995; *Yurtsev*, 2001]. The association of graminoid and forb tundra with mammoth populations is underlined by the persistence of a dwarf mammoth species on Wrangel Island into the late Holocene [*Vartanyan et al.*, 1993]. This island has retained the largest contiguous area of graminoid and forb tundra anywhere in the Arctic [*Yurtsev*, 1982], and has the highest diversity of forbs [*Lozhkin et al.*, 2001]. Our model results indicate that this kind of vegetation may have been very extensive at the LGM due to the prevalence of a dry, cold climate.

[38] Our model results do not invoke vegetation feedbacks, nor any direct influence of grazing animals on the vegetation [*Zimov et al.*, 1995], to explain the widespread distribution of graminoid and forb tundra at LGM. Nevertheless, it seems likely that more complete understanding of the high-latitude vegetation on climate at the LGM will include vegetation feedbacks [*Levis et al.*, 1999; *Chapin et al.*, 2000] and will take account of major differences in the physical characteristics of tundra biomes.

4.3. Mid-Holocene

[39] During the early and mid-Holocene the northern high latitudes were subject to greater summer and total annual insolation than present, allowing warmer than present summer temperatures to develop, particularly in continental areas (Figures 5a and 5b). Eurasia, because of its greater size, warmed more than North America during summer, and therefore the northern vegetation changes were greater in Eurasia. Simulated tree line was further north than the present in central Siberia, where the simulated summer warming was maximal according to the models. Thus a simple first-order explanation for the circumpolar asymmetry of the tree line shift, as seen both in the data and in the simulations, invokes the differential heating of the continents. However, other factors are likely to be involved, including changes in the extent and thickness of sea ice. Recent simulations have suggested that as the arctic warms, sea ice thins most rapidly in areas of ice divergence (i.e., along the central Siberian coastal region) and least rapidly in areas of ice convergence (i.e., along the northern American coastal region). As a result, changes in ice concentra-

tion are large in the eastern sector of the Arctic Ocean and there is little change in the western sector, leading in turn to larger increases in surface temperature in central Siberia than in other regions [*Vavrus*, 1999; *Hewitt et al.*, 2001; *Vavrus and Harrison*, 2003]. The southward displacement of the tree line in Québec and Labrador at that time probably reflects the localized cooling caused by the persistence of small ice sheets in this region until 5500 years BP or later [*Richard*, 1995; *Richard et al.*, 1997; *Clark et al.*, 2000]. Relicts of the Laurentide ice sheet have not been included in the climate model simulations for the mid-Holocene. This omission can explain the marked discrepancy between the observations and the model results for eastern Canada.

[40] Data and simulations agree that geographic shifts in forest type boundaries between the mid-Holocene and present were larger than the shifts in the northern forest limit. Two factors account for this phenomenon. First, there is (and presumably was throughout the Holocene) an exceptionally steep gradient in summer temperature near the Arctic coast, due to the presence of sea ice. Large changes in summer temperature are therefore required to produce a significant poleward shift in the northern forest limit from its present, near-coastal position. Second, the nature of the forest belt movements indicates winters warmer than today, e.g., in northern Europe and northern China [*Cheddadi et al.*, 1997; *Yu et al.*, 1998; *Prentice et al.*, 2000]. The "cold limit" of temperate broadleaf deciduous trees in continental regions, for example, is set by winter cold extremes, not by growing-season temperatures and their effect on NPP and tree growth. Winter temperatures in high latitudes are strongly influenced by changes in atmospheric circulation. Both factors are represented in the mid-Holocene simulations, including the simulation of a small (<2 K) winter warming in some high-latitude regions. This warming is counter to the direction of orbital forcing, which cools the simulated midlatitude winters in both models.

[41] Feedback between the land-surface and atmosphere related to forest extent at the mid-Holocene may have been overestimated in earlier work [*Foley et al.*, 1994] in light of the new data on vegetation distribution [*Bigelow et al.*, 2003; *MacDonald et al.*, 2000] which indicate a more modest tree line extension than was previously assumed. However, like earlier simulations with modern SSTs [*Texier et al.*, 1997], the simulations underestimate the observed northern treeline extension in Eurasia (Table 4). The omission of the positive feedback among forest distribution, snow albedo and sea ice [*Foley et al.*, 1994] may account for this. Vegetation feedbacks may also have contributed to mid-Holocene winter warming in the northern high latitudes [*Ganopolski et al.*, 1998].

4.4. Future Sensitivity

[42] In the future simulation, forcing by raised $[CO_2]_{atm}$ increases both winter and summer temperatures throughout the region (Figure 6). Simulated temperature anomalies in winter are generally higher than in summer, and reach >8 K in northern Beringia and on the highest-latitude land. Thus the CO_2 increase causes a large, year-round warming. The resulting combination of warmer summers and a lengthened growing season (due to higher temperatures in autumn and spring) produces a stronger effect on both GDD and NPP than warmer summers alone, and therefore a greater poleward extension of the forest limit than was shown for the mid-Holocene.

[43] The areas of perennial and seasonal sea ice in this simulation are dramatically reduced. Several studies [e.g., *Chapman and Walsh*, 1993; *Johannessen et al.*, 1995; *Maslanik et al.*, 1996; *Cavalieri et al.*, 1997; *Johannessen et al.*, 1999; *Parkinson et al.*, 1999; *Vinnikov et al.*, 1999] have confirmed an ongoing decrease in the extent of Northern Hemisphere sea ice during recent decades. Summer sea-ice extent has declined monotonically by 4 to 6% during the last 40 years [*Deser*, 2000] due to increasing late-spring temperatures, amplified by the ice-albedo feedback. This mechanism contributes to the year-round increase in simulated temperatures, and thus to the simulated expansion of forests.

[44] The simulated direct physiological effect of CO_2 on northern vegetation types was shown to be small compared to the climate effect. The response of leaf-level photosynthesis to $[CO_2]_{atm}$ concentrations is dependent on temperature: competition for Rubisco between CO_2 and O_2 is unimportant below about 15°C [*Farquhar et al.*, 1980]. This result is therefore not inconsistent with modeling studies on tropical lowland vegetation that have suggested a greater sensitivity to low CO_2 concentration [*Cowling*, 2000], or to paleodata and model results suggesting a response of tropical tree line to low $[CO_2]_{atm}$ at the LGM [*Street-Perrott et al.*, 1997; *Jolly and Haxeltine*, 1997]. It is also consistent with analyses of the recent greening trend in high latitudes, which can be explained by rising temperatures alone [*Zhou et al.*, 2001; *Kaufman et al.*, 2001; *Lucht et al.*, 2002]. The boundaries among the tundra types have been assumed to be insensitive to $[CO_2]_{atm}$.

[45] Several studies have proposed that high-latitude vegetation will gain in productivity due to increased nutrient availability as an indirect result of warming [*Chapin et al.*, 1995; *Melillo et al.*, 1993; *Oechel et al.*, 1994, 2000]. It has also been shown that the cover of shrubs and small trees has generally increased over the last 50 years [*Silapaswan et al.*, 2001; *Sturm et al.*, 2001]. BIOME4 assumes that ecosystems optimize nitrogen demand relative to supply [*Haxeltine and Prentice*, 1996b]. Increases in the productivity of cold-climate biomes are therefore simulated in concert with biome shifts in response to warming.

[46] Vegetation-atmosphere feedbacks may be important in determining the future climate. For example, *Levis et al.* [2000] showed that vegetation feedbacks under a doubled CO_2 climate could produce an additional 3 K warming during spring (April–May) in the region north of 60°N. This positive feedback would further increase the simulated temperature anomalies at high latitudes. *Chapin et al.* [2000] also identified possible vegetation changes that could result in negative feedbacks to warming, such as an shift from evergreen to deciduous forest in some regions due to drier climate conditions or increased fire frequency.

[47] Our results suggest that high-latitude ecosystems are especially sensitive to increased radiative forcing of climate due to increases in greenhouse gas concentrations. In a modeling study with the same future climate scenario, *Malcolm and Markham* [2000] projected that global ecosystem habitat loss would be greatest in Canada, Russia, and the Nordic countries. Local species loss under doubled-CO_2 climates could be as much as 20% in the cold forests

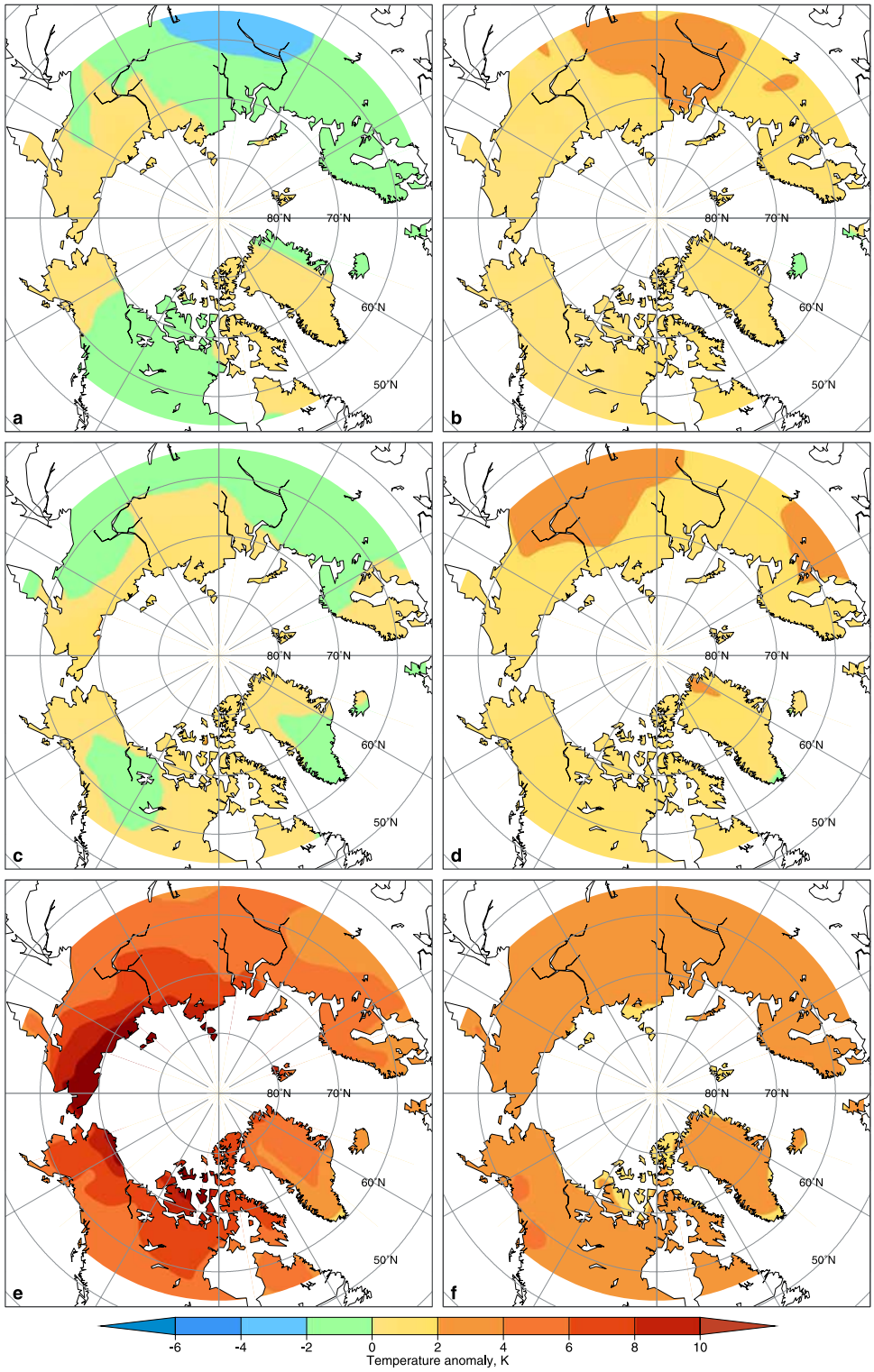

Figure 6. Mean surface air temperature anomaly in winter (December, January, February, left) and summer (June, July, August, right) for the (a, b) IPSL-CM1 mid-Holocene simulation (6000 years BP minus control), (c, d) HADCM2 mid-Holocene simulation (6000 years BP minus control), and the (e, f) HADCM2-SUL "future" simulation (the decade 2090 to 2100 minus control).

and tundra areas of the circumpolar Arctic [*Malcolm and Markham*, 2000]. Such changes would not be fully realized during this century, because the establishment and growth of trees at their climatic limit is expected to take about 200–300 years [*Chapin and Starfield*, 1997; *Cramer et al.*, 2001]. A time lag of this order has been shown in a simulation of vegetation change in the Arctic using the LPJ dynamic global vegetation model [*Kittel et al.*, 2000].

Under rapid climate change, we may also expect vegetation associations with no modern analog to form temporarily during and after the transition period, as some smaller-scale studies have reported [*Chapin and Starfield*, 1997; *Epstein et al.*, 2000]. Such phenomena also could be investigated using dynamic models.

5. Conclusions

[48] 1. The geographic distribution of high-latitude vegetation types (including the position of the forest limit, the locations of different forest types, and the diversity and distribution of tundra types) can be predicted from climatological data using a small set of PFTs. Some questions remain about how to correctly model the location of the forest limit in hypermaritime climates, and the transitions between different height classes of tundra in Canada and Siberia.

[49] 2. Palaeovegetation data, when analyzed in a globally consistent way and compared with biome model results, can be used to evaluate simulations of past climates.

[50] 3. The broad outlines of observed changes in northern high-latitude vegetation between the LGM, mid-Holocene and present are already captured by current climate models. These features include the extent of graminoid and forb tundra at the LGM, and the zonally asymmetric response of the northern forest limit to orbital forcing in the mid-Holocene.

[51] 4. Further work should include vegetation- atmosphere coupling, allowing for the different physical properties of different vegetation types (including the major differences among the tundra types). The tundra classification developed here could provide an initial basis for quantifying these properties.

[52] 5. A preliminary analysis based on a hypothetical future scenario, assuming a continuing exponential increase of $[CO_2]_{atm}$, indicates that anthropogenic warming could have a much larger effect on the forest limit and tundra ecosystems than the orbital change between mid-Holocene and present.

[53] **Acknowledgments.** The Pan-Arctic Initiative has been supported by PALE (NSF), FATE (IASC/IGBP), IGBP-GAIM, IGBP-DIS, LAII/ATLAS (NSF), PIK, and MPI-BGC. Climate model results were provided by P. Braconnot and G. Ramstein (LMD4 and LMDH), P. Valdes and B. Dong (UGAMP), A. Kitoh and H. Koide (MRI2), P. Braconnot (IPSL-CM1), C. Hewitt (HADCM2), and D. Viner (HADCM2-SUL).

References

Berger, A. L., Long-term variations of caloric insolation resulting from Earth's orbital elements, *Quat. Res.*, *9*(2), 139–167, 1978.

Berry, J., and O. Björkman, Photosynthetic response and adaptation to temperature in higher plants, *Annu. Rev. Plant Physiol. Plant Molec. Biol.*, *31*, 491–543, 1980.

Berry, J., and W. J. S. Downton, Environmental regulation of photosynthesis, in *Photosynthesis: Development, Carbon Metabolism, and Plant Productivity*, edited by Govindjee, pp. 263–343, Academic, San Diego, Calif., 1982.

Bigelow, N. H., et al., Climate change and Arctic ecosystems: 1. Vegetation changes north of 55°N between the last glacial maximum, mid-Holocene, and present, *J. Geophys. Res.*, *108*, doi:10.1029/2002JD002558, in press, 2003.

Bonan, G. B., Land atmosphere CO_2 exchange simulated by a land surface process model coupled to an atmospheric general circulation model, *J. Geophys. Res.*, *100*(D2), 2817–2831, 1995.

Braconnot, P., S. Joussaume, O. Marti, and N. de Noblet, Synergistic feedbacks from ocean and vegetation on the African monsoon response to mid-Holocene insolation, *Geophys. Res. Lett.*, *26*(16), 2481–2484, 1999.

Braconnot, P., O. Marti, S. Joussaume, and Y. Leclainche, Ocean feedback in response to 6 kyr BP insolation, *J. Clim.*, *13*(9), 1537–1553, 2000.

Braconnot, P., M. F. Loutre, B. Dong, S. Joussaume, and P. Valdes, How the simulated change in monsoon at 6 ka BP is related to the simulation of the modern climate: Results from the Paleoclimate Modeling Intercomparison Project, *Clim. Dyn.*, *19*(2), 107–121, 2002.

Braconnot, P., S. P. Harrison, S. Joussaume, C. D. Hewitt, A. Kitoh, J. Kutzbach, Z. Liu, B. Otto-Bleisner, J. Syktus, and S. L. Weber, Evaluation of coupled ocean-atmosphere simulations of the mid-Holocene, in *Past Climate Variability Through Europe and Africa*, edited by R. W. Battarbee, F. Gasse, and C. E. Stickley, Kluwer Acad., Norwell, Mass., in press, 2003.

Bradley, R. S., Past global changes and their significance for the future, *Quat. Sci. Rev.*, *19*(1–5), 391–402, 2000.

Brubaker, L. B., H. L. Garfinkel, and M. E. Edwards, A late Wisconsin and Holocene vegetation history from the central Brooks Range: Implications for Alaskan paleoecology, *Quat. Res.*, *20*, 194–214, 1983.

Cavalieri, D. J., P. Gloersen, C. L. Parkinson, J. C. Comiso, and H. J. Zwally, Observed hemispheric asymmetry in global sea ice changes, *Science*, *278*(5340), 1104–1106, 1997.

Chapin, F. S., and A. M. Starfield, Time lags and novel ecosystems in response to transient climatic change in Arctic Alaska, *Clim. Change*, *35*(4), 449–461, 1997.

Chapin, F. S., III, G. R. Shaver, A. E. Giblin, K. J. Nadelhoffer, and J. A. Laundre, Responses of Arctic tundra to experimental and observed changes in climate, *Ecology*, *76*(3), 694–711, 1995.

Chapin, F. S., III, M. S. Bret-Harte, S. E. Hobbie, and H. L. Zhong, Plant functional types as predictors of transient responses of Arctic vegetation to global change, *J. Veg. Sci.*, *7*(3), 347–358, 1996.

Chapin, F. S., III, et al., Arctic and boreal ecosystems of western North America as components of the climate system, *Global Change Biol.*, *6*(s1), 211–223, 2000.

Chapman, W. L., and J. E. Walsh, Recent Variations of sea ice and air-temperature in high latitudes, *Bull. Am. Meteorol. Soc.*, *74*(1), 33–47, 1993.

Cheddadi, R., G. Yu, J. Guiot, S. P. Harrison, and I. C. Prentice, The climate of Europe 6000 years ago, *Clim. Dyn.*, *13*, 1–9, 1997.

Christensen, T. R., S. Jonasson, T. V. Callaghan, and M. Havstrom, On the potential CO_2 release from tundra soils in a changing climate, *Appl. Soil Ecol.*, *11*(2–3), 127–134, 1999.

Christensen, T. R., T. Friborg, M. Sommerkorn, J. Kaplan, L. Illeris, H. Soegaard, C. Nordstroem, and S. Jonasson, Trace gas exchange in a high-arctic valley, 1, Variations in CO_2 and CH_4 flux between tundra vegetation types, *Global Biogeochem. Cycles*, *14*(3), 701–713, 2000.

Clark, C. D., J. K. Knight, and J. T. Gray, Geomorphological reconstruction of the Labrador Sector of the Laurentide Ice Sheet, *Quat. Sci. Rev.*, *19*(13), 1343–1366, 2000.

CLIMAP, Seasonal reconstructions of the Earth's surface as the Glacial Maximum, *Map and Chart Ser., M.C-36*, Geol. Soc. of Am., New York, 1981.

Cowling, S. A., Simulated effects of low atmospheric CO_2 on structure and composition of North American vegetation at the last glacial maximum, *Global Ecol. Biogeogr.*, *8*, 81–93, 1999.

Cowling, S. A., Plant-climate interactions over historical and geological time, Ph.D. thesis, Lund Univ., Lund, Sweden, 2000.

Cramer, W., et al., Global response of terrestrial ecosystem structure and function to CO_2 and climate change: Results from six dynamic global vegetation models., *Global Change Biol.*, *7*(4), 357–374, 2001.

de Noblet-Ducoudré, N., M. Claussen, and I. C. Prentice, Mid-Holocene greening of the Sahara: First results of the GAIM 6000 yr BP experiment with two asychronously coupled atmosphere/biosphere models, *Clim. Dyn.*, *16*, 643–659, 2000.

Denton, G. H., and T. J. Hughes, *The Last Great Ice Sheets*, John Wiley, New York, 1981.

Deser, C., On the teleconnectivity of the "Arctic Oscillation,"*Geophys. Res. Lett.*, *27*(6), 779–782, 2000.

de Vernal, A., and C. Hillaire-Marcel, Sea-ice cover, sea-surface salinity and halo-/thermocline structure of the northwest North Atlantic: Modern versus full glacial conditions, *Quat. Sci. Rev.*, *19*(1–5), 65–86, 2000.

Dong, B. W., and P. J. Valdes, Simulations of the Last Glacial Maximum climates using a general circulation model: Prescribed versus computed sea surface temperatures, *Clim. Dyn.*, *14*, 571–591, 1998.

Dyke, A. S., and V. K. Prest, The Late Wisconsinan and Holocene history of the Laurentide ice sheet, *Géogr. Phys. Quat.*, *41*(2), 237–263, 1987.

Edwards, M. E., and W. S. Armbruster, A tundra-steppe transition on Kathul Mountain, Alaska, USA, *Arct. Alp. Res.*, *21*(3), 296–304, 1989.

Ehleringer, J. R., and O. Björkman, Quantum yields for CO_2 uptake in C_3 and C_4 plants: Dependence on temperature, carbon dioxide, and oxygen concentration, *Plant Physiol.*, *59*, 86–90, 1977.

Elenga, H., et al., Pollen-based biome reconstruction for southern Europe and Africa 18,000 yr BP, *J. Biogeogr.*, *27*(3), 621–634, 2000.

Epstein, H. E., M. D. Walker, F. S. Chapin, and A. M. Starfield, A transient nutrient-based model of Arctic plant community response to climatic warming, *Ecol. Appl.*, *10*(3), 824–841, 2000.

Fairbanks, R. G., A 17,000-year glacio-eustatic sea level record: Influence of glacial melting rates on the younger dryas event and deep-ocean circulation, *Nature*, *342*, 637–642, 1989.

Farquhar, G. D., and S. von Caemmerer, Modelling of photosynthesis response to environmental conditions, in *Physiological Plant Ecology II: Water Relations and Carbon Assimilation*, edited by O. L. Lange et al., pp. 549–587, Springer-Verlag, New York, 1982.

Farquhar, G. D., S. Van Caemmerer, and J. A. Berry, A biochemical model of photosynthetic CO_2 assimilation in leaves of C_3 species, *Planta*, *149*(1), 78–90, 1980.

Farrera, I., et al., Tropical climates at the Last Glacial Maximum: A new synthesis of terrestrial palaeoclimate data, I, Vegetation, lake-levels and geochemistry, *Clim. Dyn.*, *15*, 823–856, 1999.

Felzer, B., Climate impacts of an ice sheet in East Siberia during the Last Glacial Maximum, *Quat. Sci. Rev.*, *20*(1–3), 437–447, 2001.

Fleming, K., P. Johnston, D. Zwartz, Y. Yokoyama, K. Lambeck, and J. Chappell, Refining the eustatic sea-level curve since the Last Glacial Maximum using far- and intermediate-field sites, *Earth Planet. Sci. Lett.*, *163*(1–4), 327–342, 1998.

Fleming, M. D., F. S. Chapin III, W. Cramer, G. L. Hufford, and M. C. Serreze, Geographic patterns and dynamics of Alaskan climate interpolated from a sparse station record, *Global Change Biol.*, *6*(s1), 49–58, 2000.

Foley, J. A., J. E. Kutzbach, M. T. Coe, and S. Levis, Feedbacks between climate and boreal forests during the Holocene epoch, *Nature*, *371*(6492), 52–54, 1994.

Food and Agriculture Organization, Rome, *Digital Soil Map of the World and Derived Soil Properties*, Food and Agric. Org., Rome, 1995.

Ganopolski, A., S. Rahmstorf, V. Petoukhov, and M. Claussen, Simulation of modern and glacial climates with a coupled global model of intermediate complexity, *Nature*, *391*(6665), 351–356, 1998.

Geophysical Exploration Technology, *Global DTM5*, Geophys. Explor. Technol., Leeds, UK, 1996.

Gower, S. T., J. G. Vogel, J. M. Norman, C. J. Kucharik, S. J. Steele, and T. K. Stow, Carbon distribution and aboveground net primary production in aspen, jack pine, and black spruce stands in Saskatchewan and Manitoba, Canada, *J. Geophys. Res.*, *102*(D24), 29,029–29,041, 1997.

Guiot, J., R. Cheddadi, I. C. Prentice, and D. Jolly, A method of biome and land surface mapping from pollen data: Application to Europe 6000 years ago, *Palaeoclimates*, *1*, 311–324, 1996.

Guthrie, R. D., Wooly arguments against the Mammoth Steppe: A new look at the palynological data, *Q. Rev. Archaeol.*, *6*, 9–16, 1985.

Guthrie, R. D., Origin and causes of the mammoth steppe: A story of cloud cover, woolly mammal tooth pits, buckles, and inside-out Beringia, *Quat. Sci. Rev.*, *20*(1–3), 549–574, 2001.

Guthrie, R. D., and S. Stoker, Paleoecological significance of mummified remains of Pleistocene horses from the north slope of the Brooks Range, Alaska, *Arctic*, *43*, 267–274, 1990.

Harrison, S. P., I. C. Prentice, and P. J. Bartlein, Influence of insolation and glaciation on atmospheric circulation in the North-Atlantic sector—Implications of general-circulation model experiments for the Late Quaternary climatology of Europe, *Quat. Sci. Rev.*, *11*(3), 283–299, 1992.

Harrison, S. P., G. Yu, and P. E. Tarasov, Late Quaternary lake-level record from Northern Eurasia, *Quat. Res.*, *45*, 138–159, 1996.

Harrison, S. P., J. E. Kutzbach, Z. Liu, P. J. Bartlein, B. Otto-Bliesner, D. Muhs, I. C. Prentice, and R. Thompson, Mid-Holocene climates of the Americas: A dynamical response to changed seasonality, *Clim. Dyn.*, *20*, 663–688, 2003.

Haxeltine, A., and I. C. Prentice, BIOME3: An equilibrium terrestrial biosphere model based on ecophysiological constraints, resource availability, and competition among plant functional types, *Global Biogeochem. Cycles*, *10*(4), 693–709, 1996a.

Haxeltine, A., and I. C. Prentice, A general model for the light-use efficiency of primary production, *Functional Ecol.*, *10*, 551–561, 1996b.

Henderson-Sellers, B., Calculating the surface energy balance for lake and reservoir modeling: A review, *Rev. Geophys.*, *24*(3), 625–649, 1986.

Hewitt, C. D., and J. F. B. Mitchell, A fully coupled GCM simulation of the climate of the mid- Holocene, *Geophys. Res. Lett.*, *25*(3), 361–364, 1998.

Hewitt, C. D., C. A. Senior, and J. F. B. Mitchell, The impact of dynamic sea-ice on the climatology and climate sensitivity of a GCM: A study of past, present, and future climates, *Clim. Dyn.*, *17*(9), 655–668, 2001.

Hostetler, S. W., and A. C. Mix, Reassessment of ice-age cooling on the tropical oceans and atmosphere, *Nature*, *399*, 673–676, 1999.

Hulme, M., J. Mitchell, W. Ingram, J. Lowe, T. Johns, M. New, and D. Viner, Climate change scenarios for global impacts studies, *Global Environ. Change*, *9*, S3–S19, 1999.

Hutchinson, M. F., Interpolating mean rainfall using thin plate smoothing splines, *Int. J. Geogr. Inf. Syst.*, *9*, 385–403, 1995.

Hutchinson, M. F., and R. J. Bischof, A new method of estimating the spatial distribution of mean seasonal and annual rainfall applied to the Hunter Valley, New South Wales, *Austr. Meteorol. Mag.*, *31*, 179–184, 1983.

Jacobson, G. L., and R. H. W. Bradshaw, The selection of sites for paleovegetational studies, *Quat. Res.*, *16*(1), 80–96, 1981.

Johannessen, O. M., M. Miles, and E. Bjorgo, The Arctic's shrinking sea ice, *Nature*, *376*, 126–127, 1995.

Johannessen, O. M., E. V. Shalina, and M. W. Miles, Satellite evidence for an Arctic sea ice cover in transformation, *Science*, *286*(5446), 1937–1939, 1999.

Jolly, D., and A. Haxeltine, Effect of low glacial atmospheric CO_2 on tropical African montane vegetation, *Science*, *276*, 786–788, 1997.

Joussaume, S., and K. E. Taylor, Status of the Paleoclimate Modeling Intercomparison Project (PMIP), in *Proceedings of the First International AMIP Scientific Conference, 15–19 May 1995*, edited by W. L. Gates, pp. 425–430, World Clim. Res. Prog., Monterey, Calif., 1995.

Joussaume, S., and K. E. Taylor, The Paleoclimate Modeling Intercomparison Project, in *Paleoclimate Modeling Intercomparison Project (PMIP). Proceedings of the Third PMIP Workshop.*, edited by P. Braconnot, pp. 9–24, World Meteorol. Org., World Clim. Res. Prog., La Huardière, Can., 2000.

Kageyama, M., O. Peyron, S. Pinot, P. Tarasov, J. Guiot, S. Joussaume, and G. Ramstein, The Last Glacial Maximum climate over Europe and western Siberia: A PMIP comparison between models and data, *Clim. Dyn.*, *17*(1), 23–43, 2001.

Kaplan, J. O., Geophysical applications of vegetation modeling, Ph.D. thesis, Lund Univ., Lund, Sweden, 2001.

Kaufman, Y. J., D. Tanré, O. Dubovik, A. Karnieli, and L. A. Remer, Absorption of sunlight by dust as inferred from satellite and ground-based remote sensing, *Geophys. Res. Lett.*, *28*(8), 1479–1482, 2001.

Kirschbaum, M. U. F., and G. D. Farquhar, Temperature dependence of whole-leaf photosynthesis in *Eucalyptus pauciflora* Sieb. ex Spreng., *Austr. J. Plant Physiol.*, *11*, 519–538, 1984.

Kitoh, A., A. Noda, Y. Nikaidou, T. Ose, and T. Tokioka, AMIP simulations of the MRI GCM, *Pap. Meteorol. Geophys.*, *45*, 121–148, 1995.

Kittel, T. G., W. L. Steffen, and F. S. Chapin III, Global and regional modelling of Arctic-boreal vegetation distribution and its sensitivity to altered forcing, *Global Change Biol.*, *6*(s1), 1–18, 2000.

Kohfeld, K. E., and S. P. Harrison, How well can we simulate past climates? Evaluating the models using global palaeoenvironmental datasets, *Quat. Sci. Rev.*, *19*(1–5), 321–346, 2000.

Körner, C., *Alpine Plant Life: Functional Plant Ecology of High Mountain Ecosystems*, 338 pp., Springer-Verlag, New York, 1999.

Kutzbach, J. E., and Z. Liu, Response of the African monsoon to orbital forcing and ocean feedbacks in the middle Holocene, *Science*, *278*(5337), 440–443, 1997.

Kvasov, D. D., *Late Quaternary History of Large Lakes and Inland Seas of Eastern Europe* (in Russian), 278 pp., Nauka, Leningrad, 1975.

Kvasov, D. D., *The Late-Quaternary History of Large Lakes and Inland Seas of Eastern Europe*, Ann. Acad. Sci. Fennicae, Ser. A III, Geol. Geogr., vol. 127, 71 pp., Suomalainen Tiedeakatemia, Helsinki, 1979.

Larcher, W., *Physiological Plant Ecology: Ecophysiology and Stress Physiology of Functional Groups*, Springer-Verlag, New York, 1995.

Le Treut, H., Z. X. Li, and M. Forichon, Sensitivity of the LMD general circulation model to greenhouse forcing associated with two different cloud water parameterizations, *J. Clim.*, *7*, 1827–1841, 1994.

Levis, S., J. A. Foley, and D. Pollard, CO2, climate, and vegetation feedbacks at the Last Glacial Maximum, *J. Geophys. Res.*, *104*(D24), 31,191–31,198, 1999.

Levis, S., J. A. Foley, and D. Pollard, Large-scale vegetation feedbacks on a doubled CO_2 climate, *J. Clim.*, *13*(7), 1313–1325, 2000.

Linacre, E. T., Estimating the net-radiation flux, *Agric. Meteorol.*, *5*, 49–63, 1968.

Lloyd, A. H., W. S. Armbruster, and M. E. Edwards, Ecology of a steppe-tundra gradient in interior Alaska, *J. Veg. Sci.*, *5*, 897–912, 1994.

Lozhkin, A. V., P. M. Anderson, S. L. Vartanyan, T. A. Brown, B. V. Belaya, and A. N. Kotov, Late Quaternary paleoenvironments and modern pollen data from Wrangel Island (Northern Chukotka), *Quat. Sci. Rev.*, *20*(1–3), 217–233, 2001.

Lucht, W., I. C. Prentice, R. B. Myneni, S. Sitch, P. Friedlingstein, W. Cramer, P. Bousquet, W. Buermann, and B. Smith, Climatic control of the high-latitude vegetation greening trend and Pinatubo effect, *Science*, *296*(5573), 1687–1689, 2002.

MacDonald, G. M., and K. Gajewski, The northern treeline of Canada, in *Geographical Snapshots of North America: Commerating the 27th Congress of the International Geographical Union and Assembly*, edited by D. G. Janelle, pp. 34–37, Guilford Press, New York, 1992.

MacDonald, G. M., et al., Holocene treeline history and climate change across northern Eurasia, *Quat. Res.*, *53*(3), 302–311, 2000.

Malcolm, J. R., and A. Markham, Global warming and terrestrial biodiversity decline, 23 pp., World Wildlife Fund for Nature, Gland, Switzerland, 2000.

Maslanik, J. A., M. C. Serreze, and R. G. Barry, Recent decreases in Arctic summer ice cover and linkages to atmospheric circulation anomalies, *Geophys. Res. Lett.*, *23*(13), 1677–1680, 1996.

Masson, V., S. Joussaume, S. Pinot, and G. Ramstein, Impact of parameterizations on simulated winter mid-Holocene and Last Glacial Maximum climatic changes in the Northern Hemisphere, *J. Geophys. Res.*, *103*(D8), 8935–8946, 1998.

Melillo, J. M., A. D. McGuire, D. W. Kicklighter, B. Moore, C. J. Vorosmarty, and A. L. Schloss, Global climate change and terrestrial net primary production, *Nature*, *363*(6426), 234–240, 1993.

Mitchell, J. F. B., N. S. Grahame, and K. J. Needham, Climate simulations for 9000 years before present: Seasonal variations and effect of the Laurentide ice sheet, *J. Geophys. Res.*, *93*(D7), 8283–8303, 1988.

Mix, A. C., W. F. Ruddiman, and A. McIntyre, Late Quaternary paleoceanography of the tropical Atlantic, 1, spatial variability of annual mean sea-surface temperatures, 0–20,000 years B.P., *Paleoceanography*, *1*(1), 43–66, 1986.

Neilson, R., I. Prentice, and B. Smith, Simulated changes in vegetation distribution under global warming, in *The Regional Impacts of Climate Change*, edited by R. T. Watson et al., pp. 439–456, Cambridge Univ. Press, New York, 1998.

Oechel, W. C., S. T. Hastings, G. Vourlitis, M. Jenkins, G. Riechers, and N. Grulke, Recent change of Arctic tundra ecosystems from a net carbon dioxide sink to a source, *Nature*, *361*, 520–523, 1993.

Oechel, W. C., S. Cowles, N. Grulke, S. J. Hastings, B. Lawrence, T. Prudhomme, G. Riechers, B. Strain, D. Tissue, and G. Vourlitis, Transient nature of CO_2 fertilization in Arctic tundra, *Nature*, *371*(6497), 500–503, 1994.

Oechel, W. C., G. L. Vourlitis, S. J. Hastings, R. C. Zulueta, L. Hinzman, and D. Kane, Acclimation of ecosystem CO_2 exchange in the Alaskan Arctic in response to decadal climate warming, *Nature*, *406*, 978–981, 2000.

Otto-Bliesner, B. L., El Niño/La Niña and Sahel precipitation during the middle Holocene, *Geophys. Res. Lett.*, *26*(1), 87–90, 1999.

Parkinson, C. L., D. J. Cavalieri, P. Gloersen, H. J. Zwally, and J. C. Comiso, Arctic sea ice extents, areas, and trends, 1978–1996, *J. Geophys. Res.*, *104*(C9), 20,837–20,856, 1999.

Peltier, W. R., Ice Age paleotopography, *Science*, *265*(5169), 195–201, 1994.

Pinot, S., G. Ramstein, S. P. Harrison, I. C. Prentice, J. Guiot, M. Stute, and S. Joussaume, Tropical paleoclimates at the Last Glacial Maximum: Comparison of Paleoclimate Modeling Intercomparison Project (PMIP) simulations and paleodata, *Clim. Dyn.*, *15*, 857–874, 1999.

Prentice, I. C., Records of vegetation in time and space: the principles of pollen analysis, in *Vegetation History*, edited by B. J. Huntley and T. Webb III, pp. 17–42, Kluwer Acad., Norwell, Mass., 1988.

Prentice, I. C., J. Guiot, B. Huntley, D. Jolly, and R. Cheddadi, Reconstructing biomes from palaeoecological data: A general method and its application to European pollen data at 0 and 6 ka, *Clim. Dyn.*, *12*, 185–194, 1996.

Prentice, I. C., and D. Jolly, Mid-Holocene and glacial-maximum vegetation geography of the northern continents, *J. Biogeogr.*, *27*(3), 507–519, 2000.

Prescott, J. A., Evaporation from a water surface in relation to solar radiation, *Trans. R. Soc. Sci. S. Austr.*, *64*, 114–125, 1940.

Price, D. T., D. W. McKenney, I. A. Nalder, M. F. Hutchinson, and J. L. Kesteven, A comparison of two statistical methods for spatial interpolation of Canadian monthly mean climate data, *Agric. Forest Meteorol.*, *101*(2–3), 81–94, 2000.

Ramstein, G., Y. S.-L. Treut, H. L. Treut, M. Forichon, and S. Joussaume, Cloud processes associated with past and future climate changes, *Clim. Dyn.*, *14*, 233–247, 1998.

Raynaud, D., J. Jouzel, J. M. Barnola, J. Chappellaz, R. J. Delmas, and C. Lorius, The ice record of greenhouse gases, *Science*, *259*, 926–934, 1993.

Richard, P. J. H., The vegetational cover of Québec-Labrador at 6000 years BP: An essay, *Geogr. Phys. Quat.*, *49*(1), 117–140, 1995.

Richard, P. J. H., J. J. Veillette, A. C. Larouche, B. Hetu, J. T. Gray, and P. Gangloff, Chronology of ice retreat over Gaspesie: New evidence and implications, *Geogr. Phys. Quat.*, *51*(2), 163–184, 1997.

Ritchie, J. C., Late Quaternary climatic and vegetational change in the lower Mackenzie Basin, northwest Canada, *Ecology*, *66*(2), 612–621, 1985.

Ritchie, J. C., L. C. Cwynar, and R. W. Spear, Evidence from northwest Canada for an early Holocene Milankovitch thermal maximum, *Nature*, *305*(5930), 126–128, 1983.

Rosell-Melé, A., E. Bard, K. C. Emeis, P. Farrimond, J. Grimalt, P. J. Müller, and R. R. Schneider, TEMPUS: A new generation of sea surface temperature maps, Project takes a new look at past sea surface temperatures, *Eos Trans. AGU*, *79*(33), 393–394, 1998.

Sarnthein, M., et al., Variations in Atlantic surface ocean paleoceanography, 50°–80°N: A time-slice record of the last 30,000 years, *Paleoceanography*, *10*(6), 1063–1094, 1995.

Schulze, E. D., et al., Productivity of forests in the Eurosiberian boreal region and their potential to act as a carbon sink—A synthesis, *Global Change Biol.*, *5*(6), 703–722, 1999.

Shaver, G. R., and F. S. Chapin III, Production: Biomass relationships and element cycling in contrasting Arctic vegetation types, *Ecol. Monogr.*, *61*(1), 1–31, 1991.

Silapaswan, C. S., D. Verbyla, and A. D. McGuire, Land cover change on the Seward Peninsula: The use of remote sensing to evaluate potential influences of climate change on historical vegetation dynamics, *Can. J. Remote Sens.*, *5*, 542–554, 2001.

Street-Perrott, F. A., Y. Huang, R. A. Perrott, G. Eglington, P. Barker, L. B. Khelifa, D. D. Harkness, and D. O. Olago, Impact of lower atmospheric carbon dioxide on tropical mountain ecosystems, *Science*, *278*, 1422–1426, 1997.

Sturm, M., C. Racine, and K. Tape, Increasing shrub abundance in the Arctic, *Nature*, *411*, 546–547, 2001.

Sugita, S., S. T. Andersen, M.-J. Gaillard, J. Mateus, B. V. Odgaard, I. C. Prentice, and K.-D. Vorren, Modelling and data analysis for the quantification of forest clearance signals in pollen records, *Paläoklimaforschung*, *27*, 125–131, 1998.

Svendsen, J. I., et al., Maximum extent of the Eurasian ice sheets in the Barents and Kara Sea region during the Weichselian, *Boreas*, *28*, 234–242, 1999.

Tarasov, P. E., et al., Present-day and mid-Holocene biomes reconstructed from pollen and plant macrofossil data from the former Soviet Union and Mongolia, *J. Biogeogr.*, *25*, 1029–1053, 1998.

Tarasov, P. E., et al., Last glacial maximum biomes reconstructed from pollen and plant macrofossil data from northern Eurasia, *J. Biogeogr.*, *27*(3), 609–620, 2000.

Tempo Members, Potential role of vegetation feedback in the climate sensitivity of high-latitude regions: A case study at 6000 years before present, *Global Biogeochem. Cycles*, *10*(4), 727–736, 1996.

Texier, D., N. de Noblet, S. P. Harrison, A. Haxeltine, D. Jolly, S. Joussaume, F. Laarif, I. C. Prentice, and P. Tarasov, Quantifying the role of biosphere-atmosphere feedbacks in climate change: Coupled model simulations for 6000 years BP and comparison with palaeodata for northern Eurasia and northern Africa, *Clim. Dyn.*, *13*(12), 865–882, 1997.

Tranquillini, W., *Physiological Ecology of the Alpine Timberline*, 137 pp., Springer-Verlag, New York, 1979.

Vartanyan, S. L., V. E. Garutt, and A. V. Sher, Holocene dwarf mammoths from Wrangel Island in the Siberian Arctic, *Nature*, *362*, 337–340, 1993.

Vavrus, S. J., The response of the coupled Arctic sea ice-atmosphere system to orbital forcing and ice motion at 6 kyr and 115 kyr BP, *J. Clim.*, *12*(3), 873–896, 1999.

Vavrus, S., and S. P. Harrison, The impact of sea ice dynamics on the arctic climate system, *Clim. Dyn.*, *20*, 741–757, 2003.

Vinnikov, K. Y., A. Robock, R. J. Stouffer, J. E. Walsh, C. L. Parkinson, D. J. Cavalieri, J. F. B. Mitchell, D. Garrett, and V. F. Zakharov, Global warming and Northern Hemisphere sea ice extent, *Science*, *286*(5446), 1934–1937, 1999.

Walker, D. A., Hierarchical subdivision of Arctic tundra based on vegetation response to climate, parent material and topography, *Global Change Biol.*, *6*(s1), 19–34, 2000.

Walter, H., *Vegetation of the Earth: In Relation to Climate and the Eco-Physiological Conditions*, Springer-Verlag, New York, 1973.

Webb, T., III, R. A. Laseki, and J. C. Bernabo, Sensing vegetational patterns with pollen data: Choosing the data, *Ecology*, *59*(6), 1151–1163, 1978.

Wright Jr., H. E., J. E. Kutzbach, T. Webb III, W. F. Ruddiman, F. A. Street-Perrott, and P. J. Bartlein, Global Climates since the Last Glacial Maximum, 569 pp., Univ. of Minn. Press, Minneapolis, Minn., 1993.

Young, S. B., Is steppe-tundra alive and well in Alaska?, in *Abstracts of the Fourth Biennial Meeting of the American Quaternary Association*, pp. 84–88, Arizona State Univ., Tempe, Az., 1976.

Yu, G., X. J. Sun, B. Q. Qin, C. Q. Song, H. Y. Li, I. C. Prentice, and S. P. Harrison, Pollen-based reconstruction of vegetation patterns of China in mid-Holocene, *Sci. Chin. Ser.*, *41*(2), 130–136, 1998.

Yurtsev, B. A., Relics of the xerophyte vegetation of Beringia in northeastern Asia, in *Paleoecology of Beringia*, edited by D. M. Hopkins et al., pp. 157–177, Academic, San Diego, Calif., 1982.

Yurtsev, B. A., The Pleistocene "Tundra-Steppe" and the productivity paradox: The landscape approach, *Quat. Sci. Rev.*, *20*(1–3), 165–174, 2001.

Zhou, L. M., C. J. Tucker, R. K. Kaufmann, D. Slayback, N. V. Shabanov, and R. B. Myneni, Variations in northern vegetation activity inferred from satellite data of vegetation index during 1981 to 1999, *J. Geophys. Res.*, *106*(D17), 20,069–20,083, 2001.

Zimov, S. A., V. I. Chuprynin, A. P. Oreshko, F. S. Chapin III, J. F. Reynolds, and M. C. Chapin, Steppe-tundra transition: A herbivore-driven biome shift at the end of the Pleistocene, *Am. Natural.*, *146*(5), 765–794, 1995.

P. M. Anderson, Quaternary Research Center, University of Washington, Campus Box 351360, Seattle, WA 98195-1360, USA. (pata@u.washington.edu)

A. A. Andreev, Alfred Wegner Institute for Polar and Marine Research, Forschungsstelle Potsdam, Telegrafenberg A43, D-14473 Potsdam, Germany. (aandreev@awi-potsdam.de)

P. J. Bartlein, Department of Geography, University of Oregon, Eugene, OR 97403-1251, USA. (bartlein@oregon.uoregon.edu)

N. H. Bigelow, Alaska Quaternary Center, University of Alaska, Fairbanks, P.O. Box 756960, Fairbanks, AK 99775, USA. (ffnhb@uaf.edu)

L. B. Brubaker, College of Forest Resources, University of Washington, Box 352100, Seattle, WA 98195-2100, USA. (lbru@u.washington.edu)

T. R. Christensen and B. Smith, Department of Physical Geography and Ecosystems Analysis, Lund University, Sölvegatan 13, S-223 62 Lund, Sweden. (torben.christensen@nateko.lu.se; benjamin.smith@nateko.lu.se)

W. Cramer, Potsdam Institute for Climate Impact Research, Postfach 601203, D-14412 Potsdam, Germany. (Wolfgang.Cramer@pik-potsdam.de)

M. E. Edwards, Department of Geography, University of Southampton, Southampton S09 SNH, UK. (mary.edwards@sv.ntnu.no)

S. P. Harrison and I. C. Prentice, Max Planck Institute for Biogeochemistry, Postfach 100164, D-07701 Jena, Germany. (sharris@bgc-jena.mpg.de; cprentic@bgc-jena.mpg.de)

J. O. Kaplan, Canadian Centre for Climate Modeling and Analysis, PO Box 1700 STN CSC, Victoria BC V8W 2Y2, Canada. (jed.kaplan@ec.gc.ca)

A. V. Lozhkin, Northeast Interdisciplinary Scientific Research Institute, Russian Academy of Sciences, Far East Branch, 16 Portovaya St., Magadan 685000, Russia. (lozhkin@neisri.magadan.ru)

N. V. Matveyeva and V. Y. Razzhivin, Department of Vegetation of the Far North, Komarov Botanical Institute, Popov St. 2, St. Petersburg 197376, Russia. (NadyaM@nveget.bin.ras.spb.ru; volodyar@north.bin.ras.spb.ru)

A. D. McGuire, U.S. Geological Survey, Alaska Cooperative Fish and Wildlife Research Unit, University of Alaska Fairbanks, Fairbanks, AK 99775, USA. (ffadm@uaf.edu)

D. F. Murray, University of Alaska Museum, Fairbanks, AK 99775-6960, USA. (ffdfm@uaf.edu)

D. A. Walker, Institute of Arctic and Alpine Research, University of Colorado, Boulder, CO 80309-0450, USA. (ffdaw@uaf.edu)